

# Molecular descriptors calculation as a tool in the analysis of the antileishmanial activity achieved by two series of diselenide derivatives. An insight into its potential action mechanism

María Font <sup>a,b,\*</sup>, Ylenia Baquedano <sup>b,c</sup>, Daniel Plano <sup>b,c</sup>, Esther Moreno <sup>b,c</sup>, Socorro Espuelas <sup>b</sup>, Carmen Sanmartín <sup>b,c</sup>, Juan Antonio Palop <sup>b,c</sup>

<sup>a</sup> Sección de Modelización Molecular, Departamento de Química Orgánica y Farmacéutica, Spain

<sup>b</sup> Instituto de Salud Tropical, Spain

<sup>c</sup> Sección de Síntesis, Departamento de Química Orgánica y Farmacéutica, University of Navarra, Irúnarrea, 1. E-31008 Pamplona, Spain



## ARTICLE INFO

### Article history:

Received 30 January 2015

Received in revised form 7 May 2015

Accepted 9 June 2015

Available online 18 June 2015

### Keywords:

Leishmania

Diselenide

Diselenosulfonamides

Molecular descriptors

SAR

## ABSTRACT

A molecular modeling study has been carried out on two previously reported series of symmetric diselenide derivatives that show remarkable antileishmanial *in vitro* activity against *Leishmania infantum* intracellular amastigotes and in infected macrophages (THP-1 cells), in addition to showing favorable selectivity indices. Series **1** consists of compounds that can be considered as central scaffold constructed with a diaryl/dialkylaryl diselenide central nucleus, decorated with different substituents located on the aryl rings. Series **2** consists of compounds constructed over a diaryl diselenide central nucleus, decorated in 4 and 4' positions with an aryl or heteroaryl sulfonamide fragment, thus forming the diselenosulfonamide derivatives.

With regard to the diselenosulfonamide derivatives (2 series), the activity can be related, as a first approximation, with (a) the ability to release bis(4-aminophenyl) diselenide, the common fragment which can be ultimately responsible for the activity of the compounds. (b) the anti-parasitic activity achieved by the sulfonamide pharmacophore present in the analyzed derivatives.

The data that support this connection include the topography of the molecules, the conformational behavior of the compounds, which influences the bond order, as well as the accessibility of the hydrolysis point, and possibly the hydrophobicity and polarizability of the compounds.

© 2015 Elsevier Inc. All rights reserved.

## 1. Introduction

The causative agent of the leishmaniasis, a disease with a wide range of clinical manifestations associated in humans (from self-healing skin lesions to no less than fatal visceral infection) [1–4], is made up of unicellular protozoan organisms belonging to the genus *Leishmania* (*L. donovani*, *L. infantum*, *L. major*, *L. tropica*, *L. aethiopica*, *L. brasiliensis* and *L. mexicana*, among other species [5]) that are transmitted by the bite of infected female sand-flies (*Phlebotomus* in Europe, Asia and Africa, and *Lutzomyia* in Americas). [6]

Leishmaniasis poses serious public health challenges with regard to its prevention, diagnosis, and treatment [7–9].

Chemotherapy, traditionally linked to the use of antimony-based compounds [10] (e.g., meglumine antimoniate, Glucantime ®, and sodium stibogluconate, Pentostam ®) is problematic due to the severe side effects of the few drugs that are in use; the long duration and high costs of treatment; and an increasing number of drug resistant pathogens [11–13].

With regard to obtaining new effective, safe and less expensive drugs for the treatment of infectious diseases, there are two strategies for developing new compounds that have been receiving special attention in recent years: (a) The repositioning of drugs which are already on the market for other purposes (e.g., Amphotericin B, miltefosine, pentoxifylline or tamoxifen) [14]. (b) The design of drugs that target specific metabolic pathways of the parasite, selecting an enzyme that is exclusively present in the pathogens and not in the human hosts [15].

Among the potential molecular targets, trypanothione synthetase TS $\alpha$  (EC 6.3.1.9) and trypanothione reductase TR (EC 1.6.4.8) are the most promising [16] because they are involved in the

\* Corresponding author at: Departamento de Química Orgánica y Farmacéutica, Sección de Modelización Molecular, Instituto de Salud Tropical, University of Navarra, Irúnarrea, 1, E-31008 Pamplona, Spain. Fax: +34 948 425 649.

E-mail address: [mfont@unav.es](mailto:mfont@unav.es) (M. Font).

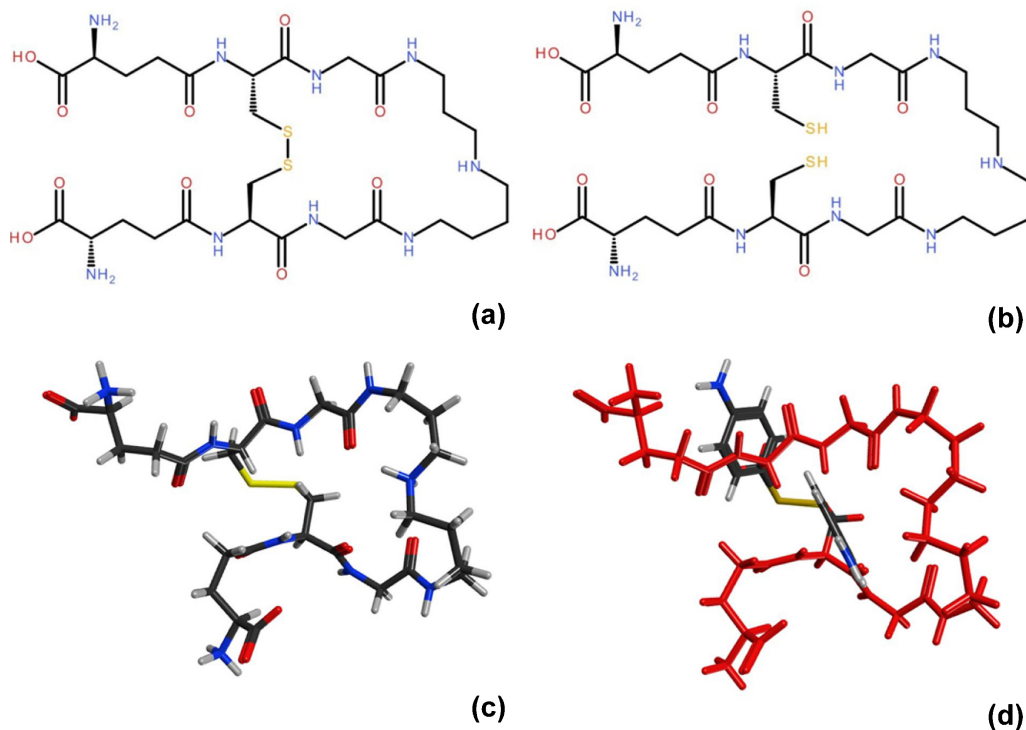


**Fig. 1.** Trypanothione (a) as disulfide T[S]2 (b) as dithiol T[SH]2 (c) 3D model for T[S]2 (isolated ligand from pdb ref 1bzl) (d) Superposition of T[S]2 and compound **1a**, taking  $\alpha$  dihedral as tether.

unique thiol-based metabolism of Leishmania, which is absent in the host. TS synthesizes  $N^1$ - $N^8$ -bis(glutathionyl) spermidine, trypanothione (Fig. 1), the main antioxidant present in Leishmania and trypanosomes [17–19] and TR keeps this molecule reduced [20]. In this respect, TR maintains the reducing environment in the protozoa by reduction of the disulfides (T[S]2, Fig. 1a and 1c) in order to maintain high levels of thiols (T[SH]2, Fig. 1b) [21].

In fact, this system replaces many of the antioxidant and metabolic functions of the glutathione (*L*- $\gamma$ -glutamyl-*L*-cysteinylglycine)/glutathione reductase (GR, EC 1.8.1.7) [22] and thioredoxin/thioredoxin reductase systems present in mammalian cells, thereby making it an essential factor for protozoa survival [23–25].

According to these considerations, TR can be considered as an effective biological target, which has been selected as the target in our seleno derivatives-based drug design strategy [26–28].

In the past few years, selenium (Se) has attracted considerable interest as a new active therapeutic tool in drug discovery. In fact, despite its interest as an essential trace element within a relatively low concentration range [29] and its demonstrated physiological role between glutathione peroxidase (GPx) components [30], Se derivatives have proven to be effective as antioxidant agents [31], acting in different therapeutic areas such as cancer prevention [32], antiviral effects [33,34], etc. These derivatives also appear to improve the immune response of the hosts against various bacterial and viral species [35,36].

We have recently reported new Se compounds with *in vitro* antiparasitic activity against *L. infantum*. Some of them possess potent activity, with selectivity indexes several-fold higher than the reference drugs miltefosine and edelfosine. In addition, their leishmanicidal activity in infected macrophages (THP-1 cells) was comparable to the effect shown by edelfosine [37–39].

Some of the aforementioned derivatives [38,39] can initially be structurally related to a central scaffold integrated by two bonded

Se atoms, decorated by two aromatic rings which carry different substituents placed in positions 2, 3 and 4 (Fig. 2).

According to the design strategy, the Se atoms present in our model, located in the central structural moiety, might interact with some nucleophilic residues located in the active enzymatic site, the sulfhydryl groups of catalytic cysteine residues Cys52 or Cys57 for example (Protein Data Bank [40] model 1TYP [41]).

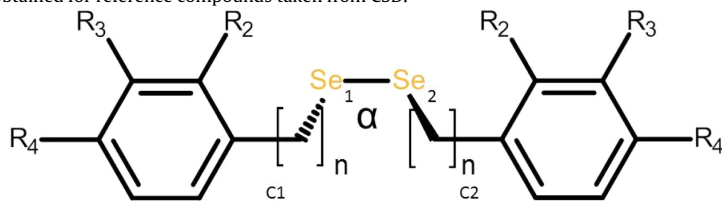
As a consequence of this nucleophilic attack, the Se–Se bond can undergo a cleavage and the selenol derivatives may also be introduced into the redox balance. The leishmanicidal activity can be finally achieved by both the direct interaction of the diseleno derivatives with the target and the possible activity of the aforementioned selenol derivatives on the redox system.

In the first design cycle [37], the objectives behind the structural variations made to the compounds in series **1** (Fig. 2a) were to evaluate: (a) the modulation of the charges and bond order values in the Se–Se bond; (b) the influence of the preferred values adopted by the central dihedral, constituted by the Se atoms and the neighbor carbon atoms, in the target activity; (c) the volume and conformational freedom of the scaffold, related with the introduction of additional methylene fragments between the central Se atoms and the lateral aromatic rings; (d) the electronic properties of the selected substituents that decorate the lateral aromatic rings, and (e) the modulation of the lipophilic characteristics as well as the overall molecular surface and volume, in order to optimize the target activity.

In the second design cycle [39], the **2** series compounds were designed (Fig. 2b). The objective underlying the structural variations performed on this series was to evaluate the effectiveness of the proposed chemical hybridization that justifies the selection of the aryl or heteroaryl sulfonic moiety as the structural modification performed on the diaryliselenide scaffold, resulting in the corresponding sulfonamides. As can be observed from the data obtained in the amastigotes test (Table 3), there is no real significant

**Table 1**

Geometrical and quantum descriptors<sup>a</sup> obtained for reference compounds taken from CSD.



Comp.	<i>n</i>	R <sub>4</sub>	R <sub>3</sub>	R <sub>2</sub>	$\alpha^b$ (°)	QSe <sub>1</sub> <sup>c</sup>	QSe <sub>2</sub> <sup>c</sup>	E <sup>d</sup>
DPHDSE02	0	H	H	H	-85.93	0.044	0.037	M
YUXPIR	0	H	H	H	88.54	0.041	0.038	P
CLPHSE	0	Cl	H	H	-86.43	0.048	0.046	M
QQQGBV01	0	CH <sub>3</sub>	H	H	89.66	0.038	0.037	P
PINTEL	0	1-Naphthyl			-85.81	0.032	0.030	M
DUWKEL	0	NO <sub>2</sub>	H	H	-98.16	0.083	0.079	M
EXUHIP	0	H	H	CH <sub>3</sub>	86.44	0.016	0.013	P
RULROG	0	H	H	CON(CH <sub>3</sub> ) <sub>2</sub>	84.50	0.085	0.006	P
YUFNOC	0	H	H	NO <sub>2</sub>	-86.30	0.126	0.089	M
HIRGIZ	0	COOH	H	H	-81.53	0.239	-0.213	M
YAWHEL	1	CH <sub>3</sub>	H	H	89.47	-0.063	-0.056	P*
IXOYAW	1	NO <sub>2</sub>	H	H	89.70	-0.027	-0.025	P*
DEMGIM	1	H	H	CH <sub>3</sub>	89.60	-0.097	-0.060	P*
KUZQUS	1	H	H	Br	90.51	-0.134	-0.070	P*

<sup>a</sup> PM3 semiempirical calculation.

<sup>b</sup>  $\alpha = C_1\text{--Se}_1\text{--Se}_2\text{--}C_2$  dihedral value.

<sup>c</sup> Selenium atomic charge (Coulson type charges).

<sup>d</sup> E=assigned enantiomer.

<sup>e</sup> P\*=proposed as P enantiomer.

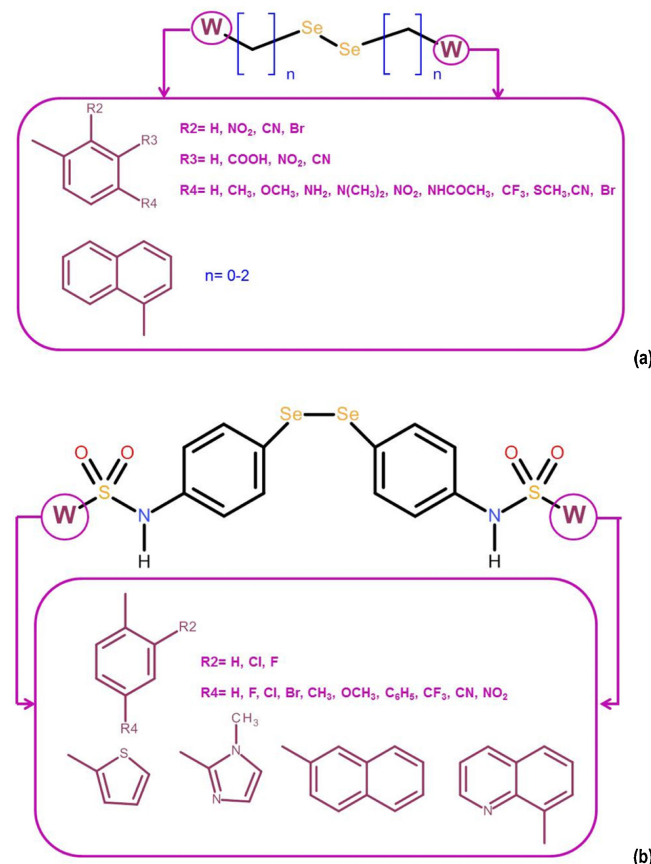


**Fig. 2.** Structural overview of the analyzed compounds (a) **1** series (b) **2** series.

difference in the activity shown by the series **2** compounds, with the possible exception of compound **2I** ( $pIC_{50} = 4.8598$ ), the less active series and compound **2p** ( $pIC_{50} = 6.0809$ ), the most active of the

compounds studied; all other compounds from the series having similar activity [39].

Taking into account this data, the following hypotheses are suggested: (a) given that the existence of a common fragment, bis(4-aminophenyl) diselenide, can be recognized in all compounds, this structure can be considered as the minimum effective fragment associated with the target activity. (b) the structural variations carried out could act as potential modulators of the cleavage of sulfonamide bonds, thereby releasing the proposed active common fragment, bis(4-aminophenyl) diselenide; thus, the **2** series derivatives may be actually considered as pro-drugs that act as carriers of the active fragment, and the variations in the target activity could then be related to the degree of ease in performing this cleavage; (c) also considering the sulfonamide moiety as an interesting structural core present in derivatives with probed antileishmanial activity [42–44], the structural variations carried out on the sulfonamide moiety can modulate the intrinsic antileishmanial activity related with this structural core. Thus, the products of series **2** could act as antileishmanial agents with two synergistic mechanisms: the controlled release of the proposed common active fragment, which in turn could interact with the parasite redox system and the basal anti-parasitic activity related with the sulfonamide pharmacophore.

**Fig. 3** shows the proposed mechanisms for series **1** and **2**.

The synthesis and the biological activities of the analyzed compounds were previously reported [37–39].

The work described here had two main goals. Firstly, to analyze the series **1** derivatives (compounds **1a–r**, **Fig. 2a**) in order to establish the corresponding structure-activity relationships that allow us to confirm the structural and conformational characteristics that comprise the fragment selected as a minimum effective structure, responsible for the target activity. This goal was achieved by the application of molecular modeling approaches in order to obtain descriptors, preferably topological and quantum descriptors, which would allow us to correlate the structural molecular variations with: (a) the degree of difficulty of the possible Se–Se bond cleavage (related to the bond order value), mediated by the aforementioned nucleophilic e attack, and subsequently, with the

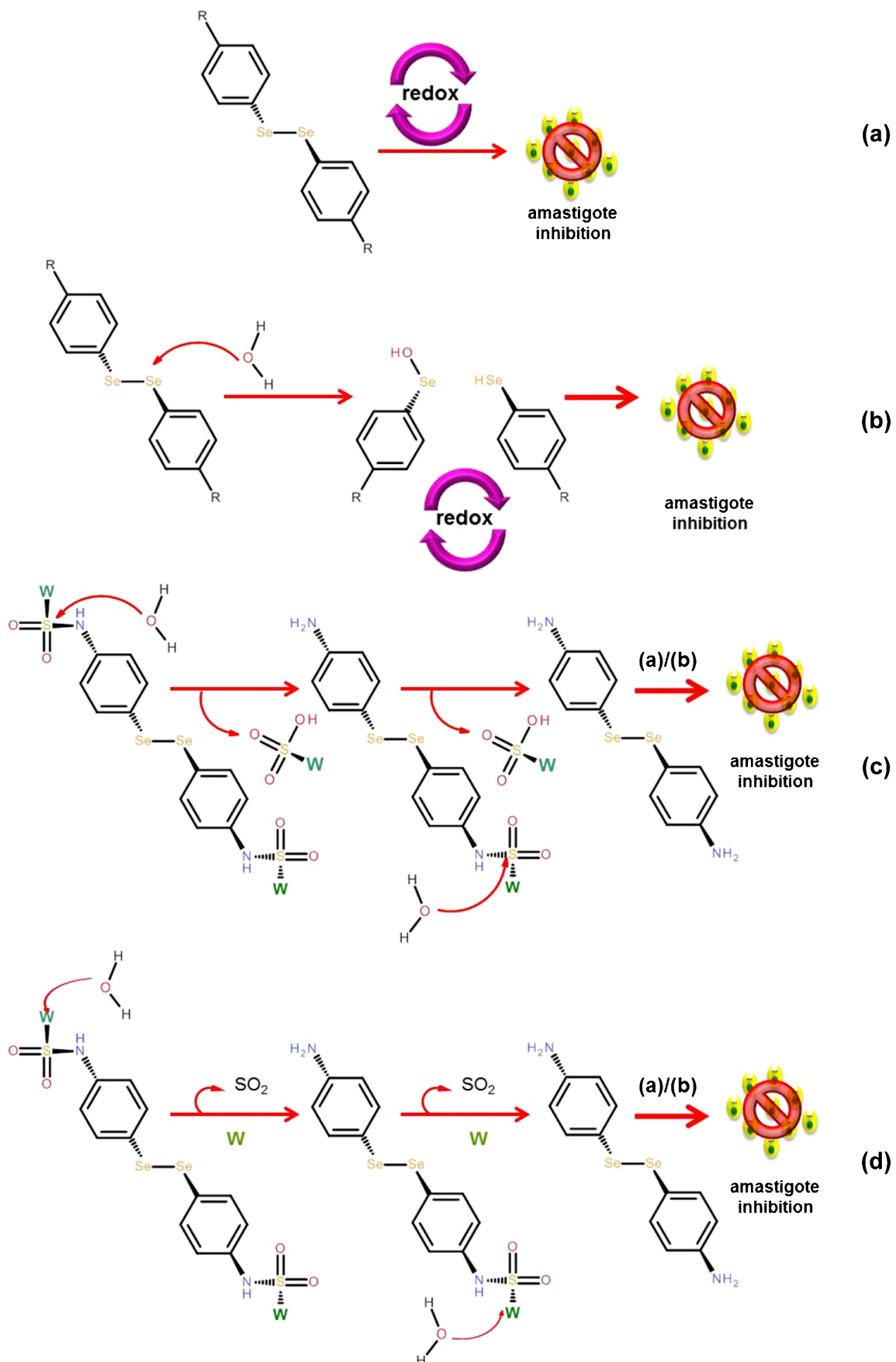


**Fig. 3.** Proposed mechanisms of action. See text for details.

activity, and (b) the conformational behavior that could facilitate the accessibility to the cleavage point.

The second goal was to study the diselenosulfonamides **2** (compounds **2a-p**, Fig. 2b) from a molecular perspective. These compounds were derivatives of compound **1a**, a compound belonging to series **1**, bis(4-aminophenyl) diselenide. The proposed approach is intended to help us to assess (a) the modulation of the S–N and S–C bond orders, with the aim of facilitating bond rupture, achieved by a nucleophilic attack [45]; (b) the conformational behavior that could facilitate the accessibility to the S–N or S–C cleavage point; and (c) the analysis of the preliminary structure–activity relationships established for the sulfonamide derivatives, considered from the whole molecule point of view and not as a sulfonamide moiety carrier or pro-drug.

The molecular modeling calculations were performed with Discovery Studio 2.5 [46], MOE (2013 and 2014 versions) [47], HyperChem v5 Pro [48] and MOPAC2009 [49] software packages.

In order to facilitate comprehension of the results concerning the effect of the structural modifications on the target activity, the previously reported activity data, expressed as  $\text{pIC}_{50}$  (M), are included in the tables. A description of the biological methods is included as supplementary material.

## 2. Results and discussion

The architecture of the analyzed compounds of the **1** series can be considered as consisting of a bis(phenyl) diselenide scaffold decorated with a series of different substituents, preferably located in position 2/2' and/or 4/4'. These substituents were selected according to: their electron-withdrawing or electron-donating profile which can modulate the Se–Se bond order; their ability to participate in the formation of intra- and intermolecular hydrogen bonds and; their ability to modulate the overall lipophilicity of the designed compounds. The introduction of one methylene fragment as a linker between the central Se atoms and the lateral rings, thereby achieving the bis(benzyl) diselenide derivatives, contributes to a significant increase of the conformational freedom and to a deep modulation of the values corresponding to the Se–Se–bond order and charges.

With regard to the compounds belonging to the **2** series, they are considered as structural derivatives of bis(4-aminophenyl) diselenide, compound **1a**, in which different aryl or heteroarylsulfonamide fragments are located in positions 4 and 4'. The nature of this moiety could have a decisive influence on the conformational behavior and therefore, on the accessibility to the point of S–N or S–C bonds cleavage, and subsequent release of the active fragment.

In the study developed in the present paper, we have selected as reference structures, a set of compounds, obtained from the Cambridge Structural Database (CSD). [50] Thus, the compounds **DPHDSE02** [51], **YUXPIR** [51], **CLPHSE** [52], **DUWKEL** [53], **QQQGBV01** [54], **PINTEL** [55], **EXUHIP** [56], **RULROG** [57], **YUFNOC** [58], **HIRGIZ** [59], **YAWHEL** [60], **IXOYAW** [61], **DEMGIM** [62], and **KUZQUS** [63] have been selected given their structural analogy with the compounds studied. (Fig. 4a-f, Table 1).

The reference CSD compounds were imported from the CSD database and transferred to the Discovery Studio 2.5 workspace in gas phase. The atom types were recognized in the implemented modified Dreiding Force Field [64] and a minimization protocol (steepest descent algorithm with a convergence criterion of  $10\text{e}^{-3}$ ) intended to eliminate tensions of the crystalline models was applied. The value of the  $\text{C}_1\text{--Se}_1\text{--Se}_2\text{--C}_2$  dihedral was calculated for each minimized conformation. These dihedral values were used as reference for the subsequent conformational behavior analysis. It is necessary to observe that due to the structural profile shown by these reference compounds, it is possible to elucidate two dif-

ferent configurations, the enantiomers M and P (see Fig. 4g for a representative image).

Then, one single point PM3 [65] calculation was applied to each of the conformations previously obtained, and the quantum reference values (charges and bond orders) were obtained.

The preliminary data, collected in Table 1, permits the obtaining of reference values for the geometrical and quantum descriptors.

Thus, the data (Table 1) concerning the CSD reference models shows the following: (a) the central dihedral adopts values within a narrow range of  $80\text{--}90^\circ$ , with negative values for the M enantiomers, and positive values for the P ones in the phenyl derivatives; the dihedral value for the reference benzyl derivatives is positive in all the analyzed cases; (b) in general, the central Se atoms show positive charges for the phenyl derivatives and negative charges for the benzyl derivatives, with a clear difference between the charges of both atoms, despite the apparent structural symmetry of the compounds.

Once the reference data were obtained, the three-dimensional models of the studied compounds were constructed in gas phase, using atoms and structural fragments from the Viewer module (DS 2.5 v), with the Dreiding Force Field. The CSD models **DPHDE02** (selected as template for the M enantiomers) and **YUXPIR** (selected as template for the P enantiomers) were used as templates for compounds **1a** and **1b** from the **1** series. Two enantiomers (M and P) have been constructed for every analyzed compound of this series

Once the starting models had been constructed, a preliminary conformational analysis was carried out. The applied protocol (Diverse Conformational Generation integrated DS 2.5 v protocol) can be summed up as follows: (a) Initial construction of the model and first minimization by application of the Dreiding minimize protocol (steepest descent algorithm with a convergence criterion of  $10\text{e}^{-3}$ ). (b) Application of the routine for conformation generation (first: conjugate-gradient minimization in torsion space; second: conjugate-gradient minimization in Cartesian space; third: Quasi–Newton minimization in Cartesian space,  $\text{rms} = 10\text{e}^{-3}$ ). (c) Elimination of the conformations whose relative energy is greater than 5 kcal/mol at a global minimum. (d) Analysis of conformational trajectory and selection of representative 100–200 lowest energy conformations for each analyzed compound (energy window = 5 kcal).

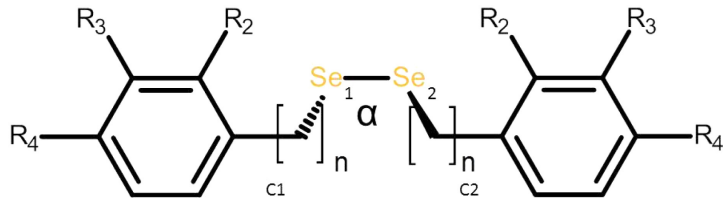
The selected conformations were included in conformational set **A** (**CSA**), and a single point PM3 calculation was performed for each included conformation (MOPAC2009 engine). The corresponding charge and bond order values were obtained, and the mean values calculated for the data obtained for each conformation, were collected.

In order to evaluate the hydrophobic profile of the analyzed compounds, the  $\text{logP}$  and  $\text{logS}$  values ( ALOGPS 2.1 online calculator [66]) were calculated as complementary data.

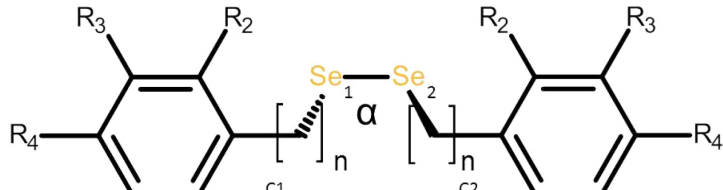
The final conformations obtained for each compound were first distributed into two configurational families, M or P, depending on the central dihedral value. In practically all the cases, a 50 % distribution of enantiomers was obtained for both families (data not shown for the sake of brevity).

The criteria for the conformation distribution in different families (Table 2), extended (A) or folded (B), have been the value (in absolute value) reached by the central dihedral angle  $\alpha$ ,  $<80^\circ$  for the A family and  $>80^\circ$  for the B one.

Thus, the preferred conformations for the less active compounds correspond to the more folded forms. As example, for compounds **1c** and **1d** the lowest energy conformations show an  $\alpha$  value ranging between 50 and  $60^\circ$  (in absolute value). This conformational behavior is conditioned by the intramolecular hydrogen bonds established between the amino and the carboxyl groups

**Table 2**Conformational behavior for series **1**.

Comp.	n	R <sub>4</sub>	R <sub>3</sub>	R <sub>2</sub>	pIC <sub>50</sub> (M)	n. conf. <sup>a</sup>	%A <sup>b</sup>	%B <sup>c</sup>
1a	0	NH <sub>2</sub>	H	H	6.1871	9	27.33	72.67
1b	0	N(CH <sub>3</sub> ) <sub>2</sub>	H	H	6.1135	12	33.32	66.68
1c	0	NH <sub>2</sub>	COOH	H	N.A. <sup>d</sup>	176	58.45	41.55
1d	0	NHCOCH <sub>3</sub>	COOH	H	N.A.	200	71.00	29.00
1e	1	NO <sub>2</sub>	H	H	6.4202	29	37.92	62.08
1f	1	H	NO <sub>2</sub>	H	4.3010	121	46.29	53.71
1g	1	H	H	NO <sub>2</sub>	6.5376	162	59.87	40.13
1h	1	Br	H	H	N.A.	14	32.87	67.13
1i	1	CF <sub>3</sub>	H	H	N.A.	50	58.00	42.00
1j	1	SCH <sub>3</sub>	H	H	N.A.	200	81.00	19.00
1k	1	CH <sub>3</sub>	H	H	N.A.	15	66.67	33.33
1l	1	CN	H	H	4.0000	25	64.00	36.00
1m	1	H	CN	H	4.3010	77	59.74	40.26
1n	1	H	H	CN	4.1249	63	66.67	33.33
1o	1	H	H	H	6.2006	15	13.33	86.67
1p	1	1-Naphthyl			N.A.	52	69.23	30.77
1q	2	NO <sub>2</sub>	H	H	N.A.	200	48.50	51.50
1r	1	OCH <sub>3</sub>	H	H	4.0000	60	60.00	40.00

<sup>a</sup> Conformational CSA set after PM3 single point calculation.<sup>b</sup> Final number of conformations for each compound (energy window = 5 kcal).<sup>c</sup> A=extended.<sup>d</sup> B=folded.**Table 3**Physicochemical and quantum descriptors<sup>a</sup> obtained for series **1**.

Comp.	pIC <sub>50</sub> (M)	n	R <sub>4</sub>	R <sub>3</sub>	R <sub>2</sub>	logP <sup>b</sup>	logS <sup>c</sup>	QSe <sub>1</sub> <sup>d</sup>	QSe <sub>2</sub> <sup>d</sup>	b.o. <sup>e</sup> .Se <sub>1</sub> —Se <sub>2</sub>	b.o. <sup>e</sup> .C <sub>1</sub> —Se <sub>1</sub>	b.o. <sup>e</sup> .Se <sub>2</sub> —C <sub>2</sub>
1a	6.1871	0	NH <sub>2</sub>	H	H	1.58	-1.88	0.020	0.021	0.94157	0.98156	0.98160
1b	6.1135	0	N(CH <sub>3</sub> ) <sub>2</sub>	H	H	3.86	-2.21	0.019	0.020	0.94021	0.98138	0.90721
1c	N.A. <sup>f</sup>	0	NH <sub>2</sub>	COOH	H	1.73	-2.16	-0.025	0.035	0.94258	0.98092	0.98054
1d	N.A.	0	NHCOCH <sub>3</sub>	COOH	H	1.16	-3.42	0.038	0.050	0.94702	0.97855	0.98125
1e	6.4202	1	NO <sub>2</sub>	H	H	3.58	-3.38	-0.010	-0.008	1.02163	0.94045	0.93915
1f	4.3010	1	H	NO <sub>2</sub>	H	3.6	-3.31	-0.018	-0.019	1.01837	0.94144	0.94148
1g	6.5376	1	H	H	NO <sub>2</sub>	3.59	-3.21	-0.004	0.017	1.02879	0.93669	0.93908
1h	N.A.	1	Br	H	H	5.46	-4.43	-0.032	-0.031	1.01390	0.93783	0.93768
1i	N.A.	1	CF <sub>3</sub>	H	H	7.11	-4.96	-0.021	-0.017	1.01972	0.93774	0.93771
1j	N.A.	1	—SCH <sub>3</sub>	H	H	4.49	-4.03	-0.030	-0.023	1.01655	0.93948	0.94066
1k	N.A.	1	CH <sub>3</sub>	H	H	4.2	-2.97	-0.044	-0.036	1.01074	0.93699	0.93510
1l	4.0000	1	CN	H	H	3.05	-3.05	-0.025	-0.022	1.01762	0.93790	0.93690
1m	4.3010	1	H	CN	H	3.02	-3.02	-0.028	-0.023	1.01606	0.93984	0.94106
1n	4.1249	1	H	H	CN	2.95	-2.97	-0.023	-0.013	1.01888	0.93778	0.94014
1o	6.2006	1	H	H	H	3.67	-2.37	-0.042	-0.033	1.01222	0.93728	0.93503
1p	N.A.	1	1-Naphthyl			5.87	-4.96	-0.044	-0.034	1.01184	0.93782	0.93656
1q	N.A.	2	NO <sub>2</sub>	H	H	4.36	-3.94	-0.038	-0.026	1.01706	0.95607	0.96071
1r	4.0000	1	OCH <sub>3</sub>	H	H	3.63	-2.76	-0.049	-0.041	1.00987	0.93791	0.93682
			R <sup>g</sup>			-0.34	0.60	<0.25	<0.25	<0.25	<0.25	<0.25

<sup>a</sup> Mean values for the conformational CSA set after PM3 single point calculation (energy window = 5 kcal).<sup>b</sup> Log of the octanol/water partition coefficient, AlogP online suite.<sup>c</sup> Log of the aqueous solubility (mol/L) AlogP online suite.<sup>d</sup> Selenium atomic charge (Coulson type charges).<sup>e</sup> b.o.=bond order.<sup>f</sup> N.A.=not active.<sup>g</sup> Regression coefficient.

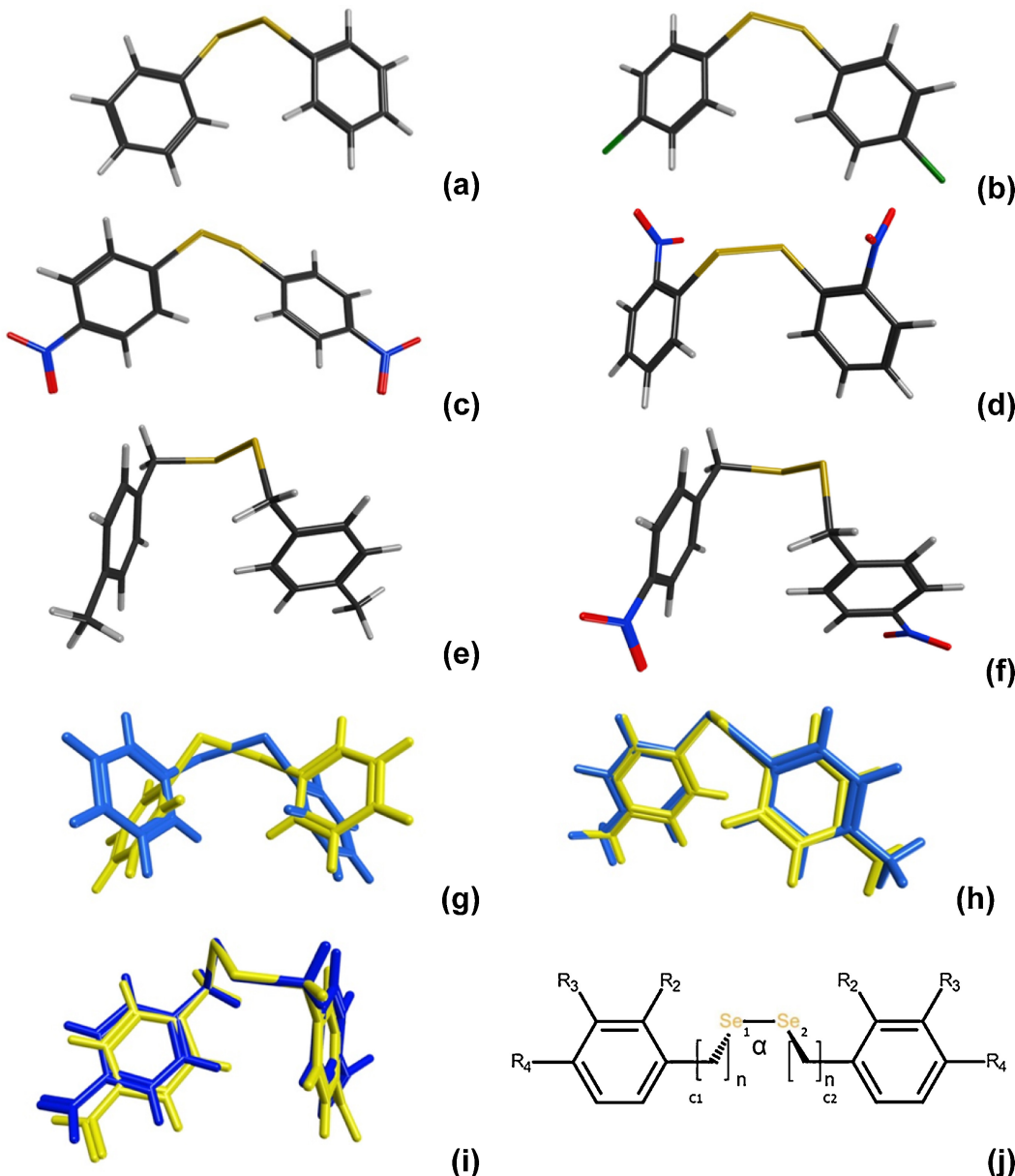


**Fig. 4.** Some CSD crystallographic structures taken as geometric references for the **1** series compounds (a) YUXPIR. (b) CLPHSE. (c) DUWKEI. (d) YUFNOC. (e) YAWHEL (f) IXOYAW. (g) Superposition of DPHDE02 (M enantiomer, in black) and YUXPIR (P enantiomer, in light grey). (h) Superposition of QQGBV01 (in black) and **1a** (in light grey, representative lowest PM3 conformation). (i) Superposition of YXOYAW (in black) and **1b** (in light grey, representative lowest PM3 conformation). (j) Selected dihedral  $\alpha_1$

that decorate the scaffold; these bonds provide additional stability in the conformations, resulting in less effective conformational freedom.

For the active compounds **1a** and **1b**, the  $\alpha$  value ranging between 90 and 95° (in absolute value). For compound **1g** the nitro substituent located in 2 and 2' positions, can establish a non-covalent intramolecular interaction between the Se atom(s) and the oxygen(s) of the nitro group, which causes this compound to preferentially adopt the extended conformation ( $\alpha$  mean value = -110.4°) with one or two of these interactions O–Se. The most active compounds belonging to the benzyl derivatives adopt preferably the extended conformation.

The rmsd value corresponding to the superposition of the representative lowest energy conformation obtained for the series 1 compounds and the reference CSD compounds (C<sub>1</sub>–Se<sub>1</sub>–Se<sub>2</sub>–C<sub>2</sub> atoms as tethers), ranges between 0.2 and 0.9 (See Fig. 4 for some representative examples).

With respect to the quantum descriptors (Table 3, mean values obtained for the conformational trajectory of each analyzed compound, CSA set, single point PM3 semi-empirical method), the atomic charge values calculated for the Se atoms show a positive value for the bisphenyldiselenide derivatives **1a–d**, whereas the bisbenzyldiselenide derivatives show negative values. In each case, an asymmetry in the charge distribution is observed.

Fig. 3 With respect to the bond order (b.o., Table 3), the value taken as a reference for the relative strength of the selected bonds, the three bonds located in the central moiety (C<sub>1</sub>–Se<sub>1</sub>–Se<sub>2</sub>–C<sub>2</sub>) were analyzed. For the bisphenyldiselenide derivatives **1a–d**, the central bond Se<sub>1</sub>–Se<sub>2</sub> is significantly weaker than C<sub>1</sub>–Se<sub>1</sub> and Se<sub>2</sub>–C<sub>2</sub> bonds. This, together with the positive value of charge of the Se atoms calculated for the **1a** and **1b** derivatives, supports our working hypothesis which claims that the central Se atoms can undergo nucleophilic attack, which results in (a) an interaction with the target, modifying its activity;(b) the cleavage of the

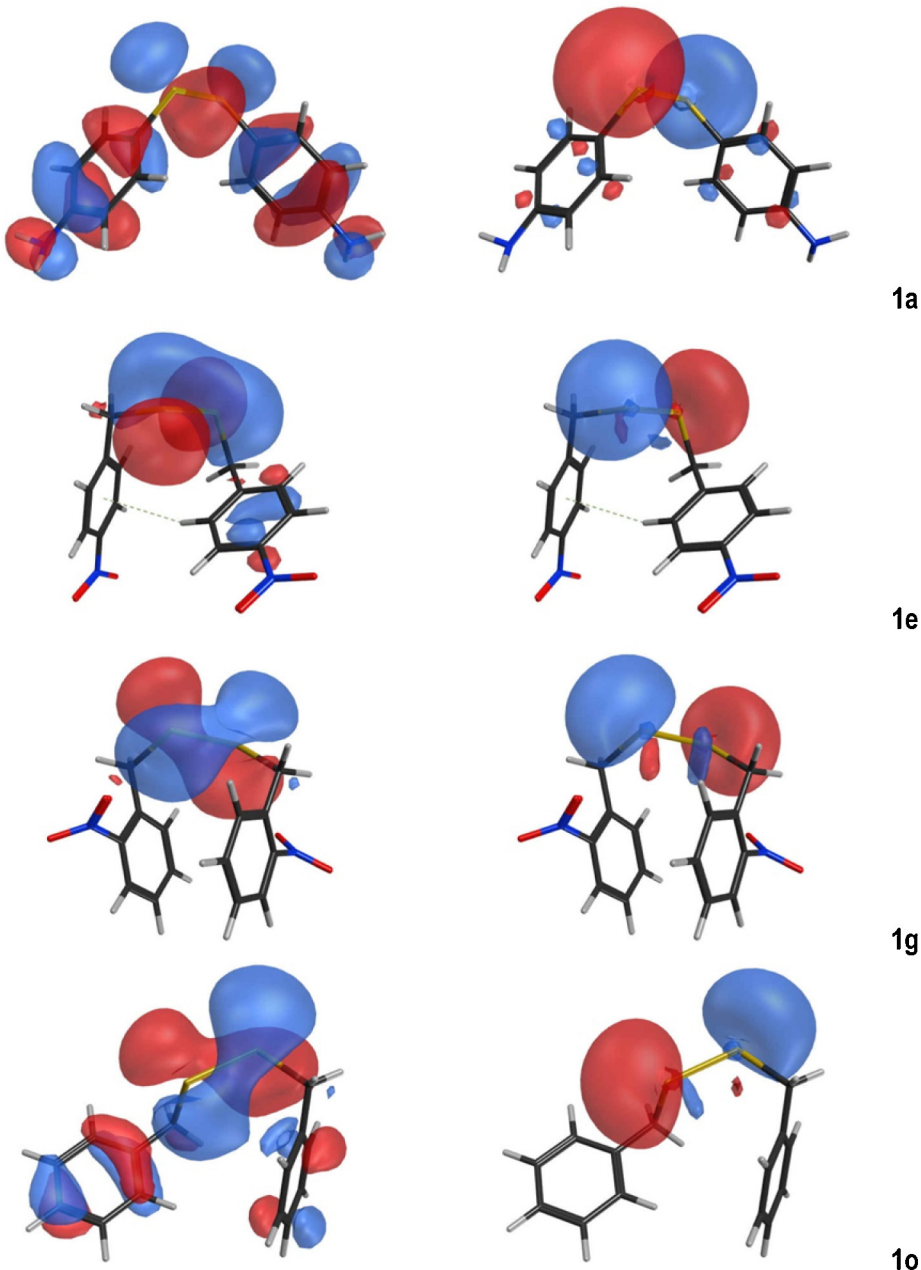


**Fig. 5.** HOMO 0 (left) and LUMO 0 (right) orbitals distribution for representative active compounds (calculated over lowest energy conformation).

Se<sub>1</sub>—Se<sub>2</sub> bond, with the corresponding release of the arylselenol derivatives (4-aminobenzeneselenol from **1a**, and 4-(dimethylamino) benzeneselenol from **1b**, respectively). These selenol derivatives, may also be involved in the redox balance, related to their potential antioxidant effect (Fig. 3a–b).

For the bisbenzyldiselenide derivatives, the bond Se<sub>1</sub>—Se<sub>2</sub> is significantly stronger than the C<sub>1</sub>—Se<sub>1</sub> and Se<sub>2</sub>—C<sub>2</sub> bonds. This, together with the negative charge value of the Se atoms calculated for the **1e–r** derivatives, suggests that bisbenzyldiselenide derivatives are not capable of undergoing the aforementioned cleavage of the Se—Se bond.

In order to elucidate the suggested implication of Se atoms in a nucleophilic attack, we provide supplementary data in which we have determined the energy values (mean values obtained for the conformational trajectory; data not shown for the sake of brevity) and the location of the HOMO 0 and LUMO 0 (calculated over the lowest energy conformation for

each compound). Some representative examples are included in Fig. 5.

The data obtained are noteworthy because all the active compounds show the LUMO 0 orbital located on the Se atoms. These data suggest that, in spite of the atomic charge and bond order values, the bisbenzyldiselenide derivatives could also undergo a nucleophilic interaction between a nucleophile and Se, but the bond cleavage proposed for the bisphenyldiselenide derivatives is not expected.

With regard to the modulation of lipophilicity, expressed by LogP (octanol/water partition coefficient) and LogS (aqueous solubility) (ALogP 2.1 online calculation, predicted values), the most active compounds show values of LogP in the range of 3–3.8, with the exception of compound **1a**, which has a value of 1.58. Despite the low regression R value ( $R=0.60$ ) obtained for the LogS predicted values, the aqueous solubility appears to be related to the activity of the compounds of this series.

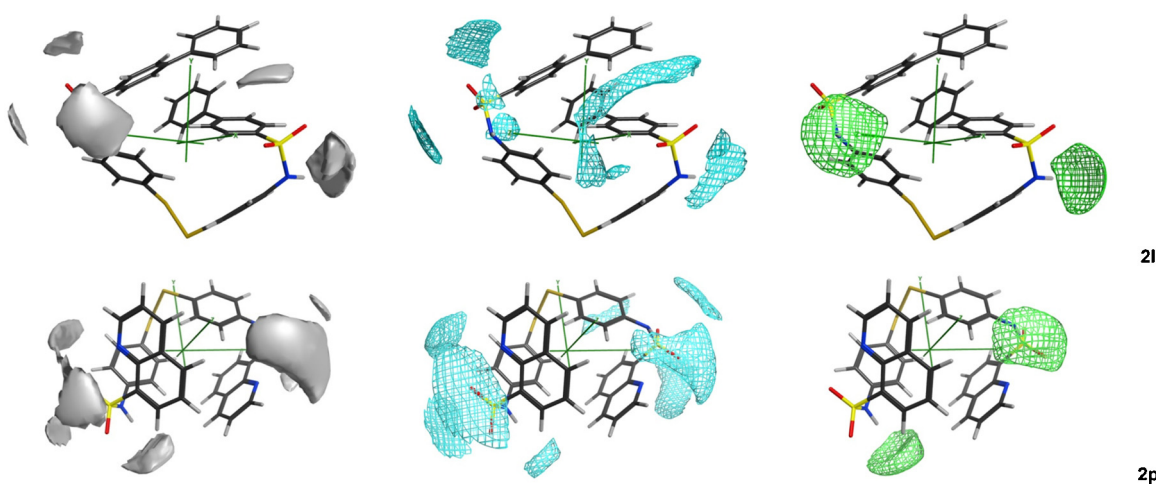
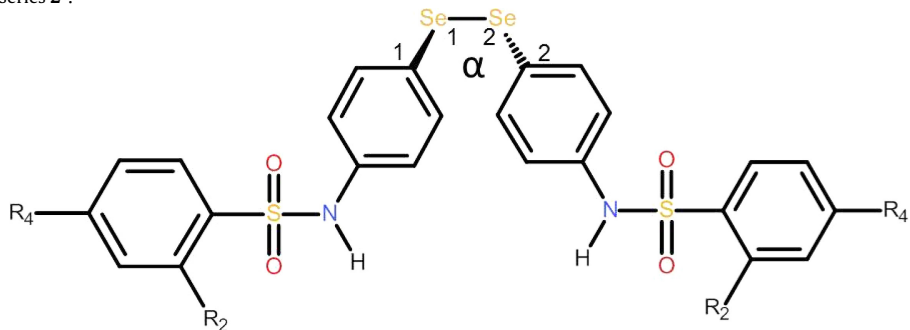


**Fig. 6.** Interaction potential map (left: O2H probe,  $-3.0 \text{ kcal/mol}$ , light grey solid volume; middle: N1 probe, amide nitrogen light grey wire mesh,  $-2.5 \text{ kcal/mol}$ ; right: O probe, oxygen carbonyl,  $-2.5 \text{ kcal/mol}$ , light grey wire mesh) for **2l**, as the least active compound, and **2p**, as representative active compound.

**Table 4**  
Conformational behavior for series **2**<sup>a</sup>.



Comp.	R <sub>4</sub>	R <sub>2</sub>	pIC <sub>50</sub> (M)	n. conf. <sup>b</sup>	%A <sup>c</sup>	%B <sup>d</sup>	%C <sup>e</sup>	Lowest conf. <sup>f</sup>
2a	H	H	5.7852	17	49.00	23.53	35.29	C
2b	CH <sub>3</sub>	H	5.8539	25	32.00	32.00	52.94	C
2c	CH <sub>3</sub> O	H	5.8861	37	40.54	29.73	29.73	B
2d	CN	H	5.7545	35	57.14	14.29	28.57	A
2e	NO <sub>2</sub>	H	5.4271	28	25.00	35.72	39.29	A
2f	CF <sub>3</sub>	H	5.6968	40	35.00	45.00	15.00	B
2g	F	H	5.8327	19	15.79	47.37	36.84	A
2h	Cl	H	5.4401	80	37.50	37.50	25.00	A
2i	Br	H	5.5528	17	29.41	29.41	41.18	C
2j	H	F	5.7799	57	26.32	17.54	56.14	B
2k	H	Cl	5.9318	28	7.14	64.29	28.57	B
2l	C <sub>6</sub> H <sub>5</sub>	H	4.8598	10	0.00	100.00	0.00	B
2m	2-thienyl		5.8125	59	35.59	47.48	16.95	C
2n	**		5.9788	33	18.18	54.55	24.24	C
2o	2-naphthyl		5.2480	20	0.00	0.00	100.00	C
2p	8-quinolyl		6.0809	20	0.00	0.00	100.00	C

\*\* = 2-(1-methyl-1H-imidazolyl).

<sup>a</sup> Conformational CSB set after PM3 single point calculation.

<sup>b</sup> Final number of conformations for each compound (energy window = 5 kcal).

<sup>c</sup> A = extended.

<sup>d</sup> B = folded.

<sup>e</sup> C = semi-folded.

<sup>f</sup> Lowest energy conformation.

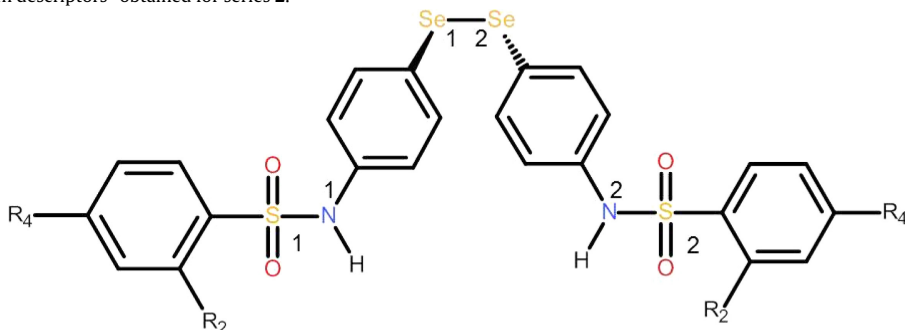
With regard to the new selenosulfonamide compounds that have been developed in the second design cycle, **series 2**, and taking into account the data previously obtained for the compounds of the first series, **series 1**, we carried out a further molecular modeling study.

As noted earlier, the derivatives belonging to the **2** series can be considered consisting of a central scaffold constructed around the **1a** compound, bis(4-aminophenyl) diselenide in which two aryl or heteroaryl fragments are located on the scaffold nitrogen

atoms. The lateral aromatic or heteroaromatic rings (monocyclic and bicyclic rings) were chosen in order to cover a wide range of electronic properties ( $\pi$ -deficient,  $\pi$  and  $\pi$ -excessive systems), surface and volume. The aim was to evaluate the ability of these features to modulate the release of the bis(4-aminophenyl) diselenide fragment, the compound **1a**, considered as the active moiety. In this way, the whole selenosulfonamide compound could be considered as a pro-drug and the aromatic or heteroaromatic moieties are considered as the release regulator elements. According to the

**Table 5**

Physicochemical and quantum descriptors<sup>a</sup> obtained for series **2**.



Comp.	<i>R</i> <sub>4</sub>	<i>R</i> <sub>2</sub>	pIC <sub>50</sub> (M)	logP <sup>b</sup>	logP <sup>c</sup>	logS <sup>d</sup>	logS <sup>e</sup>	QS <sub>1</sub> <sup>f</sup>	QS <sub>2</sub>	b.o. <sup>g</sup> S <sub>1</sub> —N <sub>1</sub>	b.o.S <sub>1</sub> —C	b.o.S <sub>2</sub> —N <sub>2</sub>	b.o.S <sub>2</sub> —C	QSe <sub>1</sub>	QSe <sub>2</sub>	b.o.Se <sub>1</sub> —Se <sub>2</sub>
2a	H	H	5.7852	4.70	4.05	-6.45	-4.86	2.278	2.278	0.70824	0.69334	0.70829	0.69315	0.038	0.038	0.94940
2b	CH <sub>3</sub>	H	5.8539	5.29	4.34	-7.40	-5.15	2.279	2.278	0.70734	0.69517	0.70723	0.69555	0.037	0.037	0.94919
2c	CH <sub>3</sub> O	H	5.8861	4.61	4.19	-6.55	-5.18	2.281	2.282	0.70741	0.69720	0.70724	0.69757	0.031	0.041	0.94906
2d	CN	H	5.7545	4.02	3.93	-7.15	-4.33	2.277	2.276	0.72203	0.67289	0.72207	0.67313	0.043	0.044	0.95458
2e	NO <sub>2</sub>	H	5.4271	4.57	4.02	-8.03	-4.95	2.276	2.276	0.71845	0.66697	0.71886	0.66715	0.048	0.049	0.95209
2f	CF <sub>3</sub>	H	5.6968	6.57	5.27	-8.56	-4.94	2.275	2.274	0.71789	0.67765	0.71791	0.67776	0.043	0.043	0.95171
2g	F	H	5.8327	5.00	4.33	-7.04	-4.51	2.282	2.281	0.71236	0.68591	0.71273	0.68598	0.042	0.042	0.95283
2h	Cl	H	5.4401	5.88	4.96	-7.92	-5.66	2.280	2.283	0.71667	0.68783	0.70972	0.69317	0.040	0.043	0.95471
2i	Br	H	5.5528	6.29	5.2	-8.63	-5.70	2.279	2.278	0.71271	0.68624	0.71263	0.68647	0.042	0.042	0.95298
2j	H	F	5.7799	5.00	4.54	-7.04	-4.40	2.287	2.281	0.71890	0.67487	0.71788	0.67849	0.037	0.040	0.95138
2k	H	Cl	5.9318	5.88	5.05	-7.92	-5.61	2.275	2.277	0.72118	0.67849	0.71775	0.68179	0.038	0.040	0.94968
2l	C <sub>6</sub> H <sub>5</sub>	H	4.8598	8.62	6.12	-11.30	-6.61	2.274	2.271	0.71447	0.68715	0.71515	0.68967	0.032	0.059	0.96122
2m	2-Thienyl		5.8125	4.42	3.89	-6.38	-3.94	2.273	2.273	0.73020	0.65493	0.72757	0.65742	0.040	0.042	0.95387
2n	**		5.9788	1.68	2.18	-4.65	-2.89	2.279	2.276	0.76440	0.64320	0.75640	0.64205	0.041	0.043	0.95768
2o	2-Naphthyl		5.2480	7.22	5.57	-10.21	-6.39	2.282	2.285	0.71322	0.69884	0.71047	0.69974	0.038	0.039	0.95128
2p	8-Quinolyl		6.0809	5.10	4.67	-7.63	-5.55	2.275	2.273	0.71371	0.69037	0.71193	0.69245	0.050	0.060	0.97530
				R <sup>h</sup>	-0.72	-0.63	0.82	0.62	<0.25	<0.25	<0.25	<0.25	<-0.25	<-0.25	<-0.25	<-0.25

\*\* = 2-(1-methyl-1H-imidazolyl).

a PM3 semiempirical single point calculation, mean values for CSB conformational set.

b Log of the octanol/water partition coefficient, MOE descriptor.

c Log of the octanol/water partition coefficient, AlogP online calculation.

d Log of the aqueous solubility (mol/L), MOE descriptor.

e Log of the aqueous solubility, AlogP online calculation.

f Atomic charge (Coulson type charges).

g b.o. = bond order.

h R = correlation coefficient.

proposed mechanism, hydrolysis can be mediated by a nucleophilic attack (mediated, for example, by a water molecule, or some nucleophilic residue located in the active site of the target enzyme) on the sulfurs that support the central scaffold or on the carbon atom near this sulfur (Fig. 3c and d).

In order to gain further insights into the structure-activity relationships that would allow us to explain the activity results, two different approaches were used to establish a preliminary SAR. Firstly, we analyzed the possible influence that structural variations carried out on the **2** derivatives have on the conformational behavior.

This was achieved by determining the conformational trajectory for each compound, the evaluation of the preferred conformations and carrying out subsequent evaluation of the accessibility to the proposed hydrolysis point, i.e., the sulfur attached to the scaffold fragment.

The second goal was to determine quantitative parameters, preferably topological and quantum parameters, which would allow us to establish a new data set to help in the further design of new molecular entities with improved activity profiles.

The models were constructed (Discovery Studio v2.5) following the same protocol used for series **1**, taking the lowest energy conformation obtained for **1a** (M enantiomer) as template. Once constructed (Dreiding FF, gas phase), and minimized (Dreiding minimize protocol), the protocol for the generation of the conformational trajectory for each **2** compound was applied.

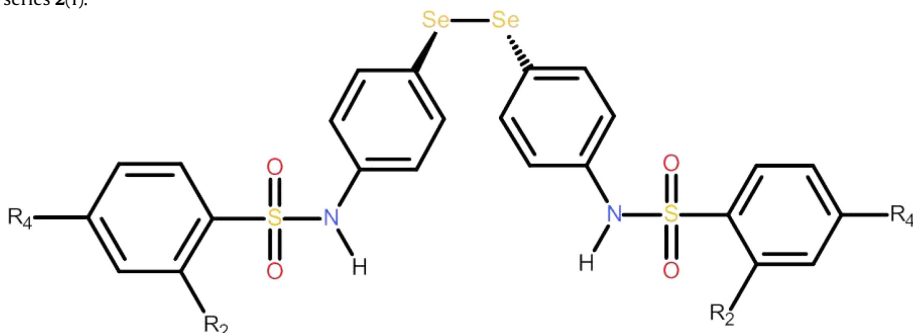
The low energy conformations obtained (energy window = 5 kcal, 200 as maximum conformation number) for the **2** derivatives were included in the conformational set **CSB**.

A single point PM3 calculation for each conformation was carried out and the charge, bond order and mean polarizability values were obtained.

Finally, among the conformations included in the CSB set, five representative low energy conformations for each compound were selected and included in the conformational set **CSC**. A single point Ab Initio STO-3G was applied to these conformations and the mean polarizability values were calculated.

The conformational behavior for the derivatives of the **2** series is summarized in Table 4. The final conformations obtained for each compound were first distributed into families, according to the central α dihedral value, in three families A (extended), B (folded) and C (semifolded).

In some instances the semifolded conformations are stabilized by the formation of intramolecular hydrogen bonds and/or H–arene interactions. Thus, in compound **2p**, the most active compound from the **2** series, the lowest energy conformations show a strong hydrogen bond established between the nitrogen present in the quinolyl ring and the hydrogen of the sulfonamide moiety, which could lead to an increased exposure of the sulfur atoms. In a similar way, the most active compounds, **2c**, **2m** and **2n** showed hydrogen bonds in their lowest energy conformations, established between the hydrogen of the sulfonamide moiety and heteroatoms present in the substituent located in 4 or 4' positions.

**Table 6**2D Descriptors<sup>a</sup> obtained for series 2(I).

Comp.	R <sub>4</sub>	R <sub>2</sub>	pIC <sub>50</sub> (M)	glob	apol	mr	SMR	SlogP	chi1v	Kier2	petitjean	petitjeanSC	diam <sup>b</sup>	rad <sup>c</sup>
2a	H	H	5.7852	0.1841	74.32386	14.56311	13.81610	2.562	19.03491	12.49704	0.47619	0.90909	21	11
2b	CH <sub>3</sub>	H	5.8539	0.2260	80.51103	15.47057	14.76350	3.179	19.85628	12.90179	0.47826	0.91667	23	12
2c	CH <sub>3</sub> O	H	5.8861	0.2291	82.11503	15.85171	15.12650	2.580	20.08102	14.25446	0.48000	0.92308	25	13
2d	CN	H	5.7545	0.2057	78.71027	15.74628	14.75910	2.306	19.80349	14.25446	0.48000	0.92308	25	13
2e	NO <sub>2</sub>	H	5.4271	0.2105	78.39828	15.57908	15.14698	2.379	20.03379	14.65036	0.48000	0.92308	25	13
2f	CF <sub>3</sub>	H	5.6968	0.2373	79.85227	15.67582	14.83990	5.223	20.49017	14.18685	0.48000	0.92308	25	13
2g	F	H	5.8327	0.2012	74.10427	14.67690	13.80770	2.841	19.23424	12.90179	0.47826	0.91667	23	12
2h	Cl	H	5.4401	0.1954	77.35027	15.53915	14.81810	3.869	19.99017	12.90179	0.47826	0.91667	23	12
2i	Br	H	5.5528	0.2020	79.09027	16.03862	15.35610	4.087	20.82024	12.90179	0.47826	0.91667	23	12
2j	H	F	5.7799	0.2133	74.10427	14.68438	13.80770	2.841	19.24621	12.90179	0.47619	0.90909	21	11
2k	H	Cl	5.9318	0.1925	77.35027	15.54663	14.81810	3.869	20.00214	12.90179	0.47619	0.90909	21	11
2l	C <sub>6</sub> H <sub>5</sub>	H	4.8598	0.2819	100.77821	19.55983	18.90330	5.896	23.17765	16.80556	0.48276	0.93333	29	15
2m	2-Thienyl		5.8125	0.1951	70.41669	14.19885	13.39150	2.685	19.76319	11.16000	0.47368	0.90000	19	10
2n	**		5.9788	0.1743	71.68386	13.97378	13.22550	0.748	18.70186	11.58848	0.47368	0.90000	19	10
2o	2-Naphthyl		5.2480	0.2735	91.07103	17.79318	17.31730	4.869	21.84431	14.18685	0.48000	0.92308	25	13
2p	8-Quinolyl		6.0809	0.1442	88.41744	17.47619	16.87630	3.659	21.57587	14.18685	0.47826	0.91667	23	12
<i>R</i> <sup>d</sup>			-0.76	-0.64	-0.66	-0.67	-0.63	-0.67	-0.63	-0.64	-0.64	-0.69	-0.69	-0.69

\*\* = 2-(1-methyl-1H-imidazolyl).

<sup>a</sup> Values obtained for CSB conformational set.<sup>b</sup> diam. = diameter.<sup>c</sup> rad. = radius.<sup>d</sup> *R* = correlation coefficient.

From this initial study, it can be proposed that in the more active compounds, the lowest energy conformations show a pattern of intramolecular interactions which favors the point of hydrolysis, the sulfonamide moiety, being more exposed to nucleophilic attack, a situation that results in an increased release of **1a**.

In order to confirm the above conclusion, the interaction map of the molecular surface was also calculated for each compound by using an O2H probe (0.00 charge, with an interaction energy of -3.0 kcal/mol), a N1 probe (amide nitrogen, -2.5 kcal/mol), and an O probe (oxygen carbonyl, -2.5 kcal/mol). The graphical representation showing where these chemical probes have favorable interactions with the molecular surface, calculated according to Goodford's GRID approach [67], confirms that the most favorable interactions were shown by compounds **2d**, **2e**, **2g**, **2m**, **2n** and **2p** (see Fig. 6 for representative examples). In these cases, the interaction map with the O2H probe is located close to the S that bears the sulfonamide moiety and to the neighbor C, i.e., the proposed hydrolysis points.

It can be observed in Fig. 6 that the less active compound, **2l**, has an interaction area with the O2H probe that is smaller than that which was obtained for the most active compounds.

In order to obtain new data that would allow us to correlate the molecular structural variations with the antileishmanial activity, a further strategy has been developed, aimed at obtaining a set of descriptors, preferably physicochemical and topological descriptors.

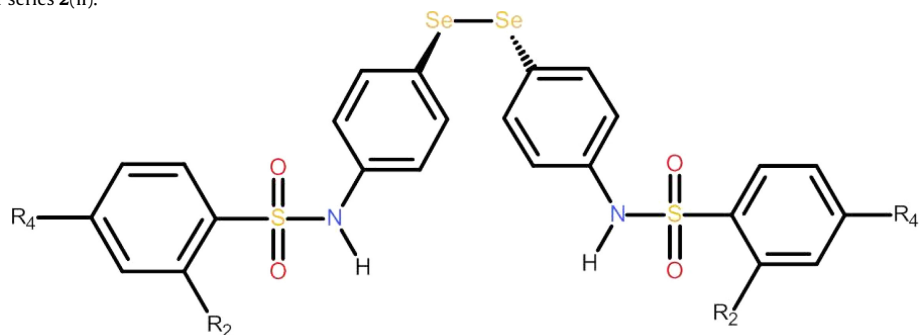
The conformations of the CSB were imported into the MOE2014 workspace. The descriptors implemented in the MOE suite were calculated for the aforementioned CSB set (see supplementary material section). The final value for the conformationally depend-

ent descriptors presented in the tables represents the mean value calculated with the data obtained for each conformation. Thus, we calculated a significant number of 2D and 3D molecular descriptors with the aim of obtaining data that would allow us to evaluate topological, hydrophobic and electrostatic aspects. Data obtained in the first design cycle and the ones obtained for the currently analyzed sulfonamide derivatives which are related to the accessibility of the hydrolysis point were also considered when selecting the descriptors.

The small number of compounds that comprise this series and the large number of analyzed parameters (see Supplementary material section) required us to perform an initial regression analysis and a Principal Components Analysis [68] (data not shown for the sake of brevity, see supplementary material section for details). This process allowed us to detect the descriptors that are likely to be more important in establishing structure-activity relationships.

The descriptors for which we obtained the best correlation values (*R*>0.6) are shown in Tables 5–9.

The descriptors can be grouped as follows: (a) Physical properties, shape and hydrophobicity descriptors: apol [69] (Sum of atomic polarizabilities, including implicit hydrogens); glob (Molecular globularity, or inverse condition number, smallest eigenvalue divided by the largest eigenvalue, of the covariance matrix of atomic coordinates. A value of 1 indicates a perfect sphere while a value of 0 indicates a two- or one-dimensional object.); Polarizability (mean polarizability) calculated by PM3 semiempirical approach and STO-3G Ab initio approach; logP, SlogP (log of the coefficient octanol/water partition) and logS, (log of the aqueous solubility) calculated by MOE software [70] and AlogP 2.1 online calculation; pmi1 (Principal moment of inertia 1); npr1

**Table 7**2D Descriptors<sup>a</sup> obtained for series **2(II)**.

Comp.	R <sub>4</sub>	R <sub>2</sub>	pIC <sub>50</sub> (M)	PEOE.VSA.NEG	VDistEq	vdw.area	vdw.vol	W.Path <sup>b</sup>
2a	H	H	5.7852	261.22076	4.16075	491.19336	642.32703	4459
2b	CH <sub>3</sub>	H	5.8539	278.62341	4.25140	525.65753	691.18536	5272
2c	CH <sub>3</sub> O	H	5.8861	241.71848	4.34252	555.66498	712.50812	6205
2d	CN	H	5.7545	272.19595	4.34252	538.65387	693.18719	6205
2e	NO <sub>2</sub>	H	5.4271	255.55345	4.40397	547.47003	690.13110	7192
2f	CF <sub>3</sub>	H	5.6968	308.16278	4.44703	552.11267	710.03882	8233
2g	F	H	5.8327	260.52823	4.25140	500.01172	648.61151	5272
2h	Cl	H	5.4401	295.87488	4.25140	526.35614	674.23889	5272
2i	Br	H	5.5528	323.96066	4.25140	549.90686	700.30212	5272
2j	H	F	5.7799	285.03806	4.18753	500.01172	648.61151	5156
2k	H	Cl	5.9318	320.38467	4.18753	526.35614	674.23889	5156
2l	C <sub>6</sub> H <sub>5</sub>	H	4.8598	368.09418	4.59632	632.18982	872.27478	10801
2m	2-Thienyl		5.8125	240.66309	4.07511	472.53766	601.17950	3752
2n	**		5.9788	199.05650	4.11297	511.43454	622.92670	4401
2o	2-Naphthyl		5.2480	319.07455	4.40891	566.10864	786.36145	8031
2p	8-Quinolyl		6.0809	297.09573	4.32742	562.39728	768.21033	7775
	R <sup>c</sup>		-0.62	-0.68	-0.64	-0.65	-0.65	

\*\* = 2-(1-methyl-1H-imidazolyl).

<sup>a</sup> Values obtained from CSB set.<sup>b</sup> W.Path = Weiner path.<sup>c</sup> R = correlation coefficient.

(normalized PMI ratio); MR and SMR (Molecular refractivity, including implicit hydrogens); vol (van der Waals volume in Å<sup>3</sup> calculated using a grid approximation) and vdw.vol (Van der Waals volume in Å<sup>3</sup> calculated using a connection approximation); PEOE\_VSA\_NEG (total negative van der Waals surface area in Å<sup>2</sup>); VSA (van der Waals surface in Å<sup>2</sup> calculated using a grid approximation) and vdw\_area (Van der Waals surface area in Å<sup>2</sup> calculated using a connection approximation); vsurf\_V (Surface interaction); vsurf\_EDminn (Lowest hydrophobic energy). (b) Topological information indices (Adjacency and Distance Matrix Descriptors): chi1\_v (Atomic valence connectivity index, order 1), chi1v\_C (Carbon valence connectivity index, order 1) and chi1\_C (Carbon connectivity index, order 1) [71,72]; diameter [73] (Largest vertex eccentricity in graph); Kier2 and KierA2 [71] (Second kappa shape index); petitjean and petitjeansC [73] ([diameter - radius] / diameter); radius [73] (Smallest vertex eccentricity in graph); std\_dimn (Standard dimension n: the square root of the n largest eigenvalue of the covariance matrix of the atomic coordinates. A standard dimension is equivalent to the standard deviation along a principal component axis); weinerPath [74,75] (Weiner path number, half the sum of all the distance matrix entries). (c) PM3-LUMO 0 (LUMO 0 orbital location). The data concerning the atomic charges for Se and S atoms and the Se-Se, S-N, S-C b.o. are included in Table 5, for comparative purposes.

With regard to the modulation of lipophilicity, expressed by the LogP, LogS and SlogP values (Tables 5 and 6), a clear correlation among the solubility in water and the biological activity is detected. In fact, the most active compound, **2p**, shows a moderate solubility related to its lower lipophilicity whereas the less active one, **2l**, shows higher lipophilic character.

Another data related with the positive R obtained for some descriptors such as vsurf\_EDmin1, vsurf\_EDmin2 and vsurf\_EDmin3, descriptors (Table 8) that are related with the lowest hydrophobic energy, is that they appear to confirm the importance of the whole hydrophobic nature of the molecules in the target activity.

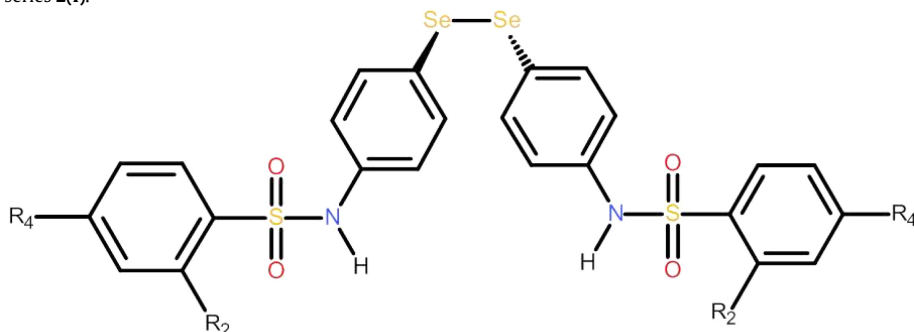
With respect to the polarizability, expressed as apol, MR, SMR (Table 6) and mean polarizability (Table 9), a correlation is shown. In fact, compound **2l**, the less active one of series 3, has a mean polarizability value, calculated by both PM3 and Ab initio methods, which is the lowest of those obtained for the entire series. With respect to the apol, MR and SMR values, a negative correlation is observed because the values that were obtained are significantly higher than those obtained for the most active compounds. These data, along with the values of diameter (diam.) and radius (Table 6) obtained for these compounds (descriptors that also have a negative R coefficient), permit the proposal of a possible relationship among the polarizability, the molecular shape and the biological activity related with the accessibility of the cleavage points.

With regard to the rest of the 2D topological descriptors calculated (Tables 6 and 7), the data that was obtained, in spite of the relatively low quality of R obtained, lead us to emphasize the importance of the topological features on the biological activity. In fact, all the regression coefficient values are negative.

The different 2D and 3D descriptors related to the different values of the areas and volumes of the analyzed derivatives (Tables 7 and 8) show negative R values.

Considering these data, together with the aforementioned comments related to polarizability, allow us to state that as polarizability increases, the dispersion forces also become stronger;

**Table 8**  
3D Descriptors<sup>a</sup> obtained for series 2(I).



Comp.	R <sub>4</sub>	R <sub>2</sub>	pIC <sub>50</sub> (M)	vol	VSA	vsurf_V	vsurf.EDmin1	vsurf.EDmin2	vsurf.EDmin3
2a	H	H	5.7852	522.875	575.704	1103.12931	-3.04208	-2.97433	-2.92994
2b	CH <sub>3</sub>	H	5.8539	499.000	554.736	1171.14904	-3.12685	-3.04696	-2.98630
2c	CH <sub>3</sub> O	H	5.8861	475.875	526.148	1183.11473	-3.34764	-3.25950	-3.18695
2d	CN	H	5.7545	520.250	580.314	1182.01786	-3.30445	-3.22787	-3.17722
2e	NO <sub>2</sub>	H	5.4271	506.625	564.454	1189.59451	-3.38520	-3.27091	-3.20492
2f	CF <sub>3</sub>	H	5.6968	505.125	562.529	1204.75000	-3.06877	-2.97270	-2.91363
2g	F	H	5.8327	469.375	521.120	1101.53947	-3.21034	-3.14453	-3.09034
2h	Cl	H	5.4401	517.750	580.294	1149.95982	-3.36534	-3.29080	-3.22638
2i	Br	H	5.5528	504.875	561.895	1181.12838	-3.38293	-3.26381	-3.19659
2j	H	F	5.7799	567.250	608.372	1099.44612	-3.06871	-2.99273	-2.92642
2k	H	Cl	5.9318	553.250	588.445	1144.61250	-3.14695	-3.07914	-3.01293
2l	C <sub>6</sub> H <sub>5</sub>	H	4.8598	631.625	682.603	1384.98214	-3.60891	-3.51274	-3.46554
2m	2-Thienyl		5.8125	461.500	518.523	1046.65074	-3.20971	-3.12640	-3.05885
2n	**		5.9788	449.000	499.895	1063.11719	-3.30785	-3.21016	-3.15110
2o	2-Naphthyl		5.2480	497.375	545.449	1210.50000	-3.36940	-3.17985	-3.05898
2p	8-Quinolyl		6.0809	472.125	523.128	1216.25000	-3.16989	-3.09609	-3.06113
	<i>R</i> <sup>b</sup>		-0.68	-0.70	-0.68	0.72	0.67	0.62	

\*\* = 2-(1-methyl-1H-imidazolyl).

<sup>a</sup> Mean values obtained from the PM3 single point conformations CSB set.

<sup>b</sup> *R* = correlation coefficient.

the molecules with higher polarizability values can attract one another more vigorously, but this feature also affects dispersion forces through the molecular shape, area and volume of the affected molecules.

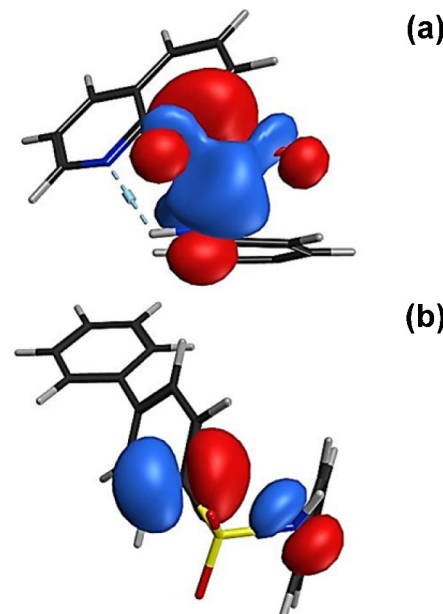
Other 3D descriptors, such as globularity (glob., Table 9), show that the more active compounds, with lower globular character and with lower volume and surface values, can actually be considered as being more elongated molecules, whereas the compounds that preferably adopt a more compact conformation have decreased activity.

With respect to the proposed mechanism related to the release of the scaffold, (Fig. 3c and d), the data obtained in relation to the partial charge on the sulfurs (Table 5) show large positive charge values for both atoms (significantly larger values than those obtained for Se atoms), with a slight difference among the values for both atoms S<sub>1</sub> and S<sub>2</sub>. The larger partial positive charge on the S in sulfonamide moiety can attract the partial negative charge on water, or on another nucleophilic group such as the sulphydryl group, making the proposed nucleophilic attack easier.

With regard to the S–N b.o. (Table 5), the values are collected in a range of 0.70–0.76, values which are significantly lower than those obtained for the Se–Se bond (range of 0.94–0.98). With respect to the S–C b.o., the values obtained are even lower than those for the S–N bonds (range 0.67–0.69).

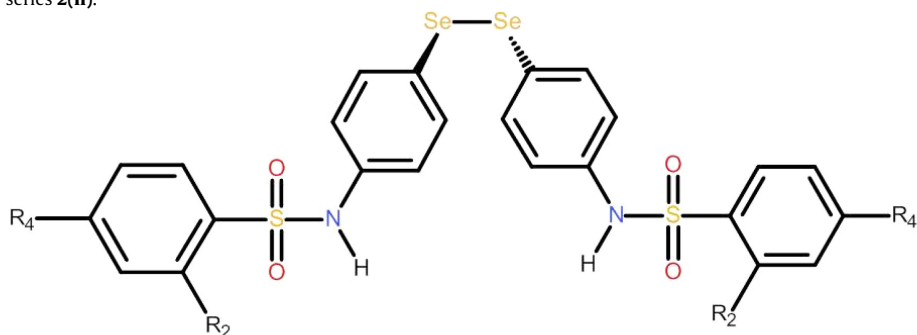
Taking into account all these aforementioned data, it can be argued that when the nucleophilic attack on sulfur occurs, both S–N and S–C bonds are most likely liable to break, with a possible preference for the latter bond.

In order to elucidate the suggested implication of S atoms in a nucleophilic attack, we have provided supplementary data showing that we have determined the energy values (mean values



**Fig. 7.** LUMO 0 location on sulfonamide moiety (a) Compound 2p taken as representative active compound (b) Compound 2l, taken as the least active compound. See text for details.

obtained from the CSB conformational set; data not shown for the sake of brevity) and location of the HOMO 0 and LUMO 0 for each compound (calculated over one representative lowest energy conformation selected from the CSB set). Some representative

**Table 9**3D Descriptors<sup>a</sup> obtained for series **2(II)**.

Comp.	R <sub>4</sub>	R <sub>2</sub>	pIC <sub>50</sub> (M)	glob	npr	pmi1	std.dim2	std.dim3	Mean.pol (PM3)	Mean.pol (STO-3G) <sup>b</sup>
2a	H	H	5.7852	0.1841	0.28020	4438.33276	2.09563	1.42123	335.618	225.540
2b	CH <sub>3</sub>	H	5.8539	0.2260	0.30160	4969.68898	2.23983	1.53189	354.207	249.950
2c	CH <sub>3</sub> O	H	5.8861	0.2291	0.39713	5737.80638	2.28534	1.64081	330.650	263.890
2d	CN	H	5.7545	0.2057	0.32154	5321.78151	2.12889	1.49164	324.600	232.880
2e	NO <sub>2</sub>	H	5.4271	0.2105	0.33066	5797.11386	2.16132	1.49209	343.875	285.290
2f	CF <sub>3</sub>	H	5.6968	0.2373	0.33781	6732.50233	2.26702	1.51404	380.341	252.770
2g	F	H	5.8327	0.2012	0.33724	5184.94985	2.10216	1.45859	349.339	280.030
2h	Cl	H	5.4401	0.1954	0.39373	5795.85509	2.15570	1.48247	330.657	222.530
2i	Br	H	5.5528	0.2020	0.37554	6663.20706	2.13010	1.46906	342.418	227.500
2j	H	F	5.7799	0.2133	0.32015	4850.87531	2.07327	1.45203	281.452	237.440
2k	H	Cl	5.9318	0.1925	0.33977	5263.54426	2.14612	1.47520	285.012	251.500
2l	C <sub>6</sub> H <sub>5</sub>	H	4.8598	0.2819	0.55487	8439.93914	2.71697	1.76581	152.818	137.250
2m	2-Thienyl		5.8125	0.1951	0.39698	4883.27583	2.19824	1.41790	385.192	265.540
2n	**		5.9788	0.1743	0.39117	4809.14341	2.22295	1.45720	382.922	382.920
2o	2-Naphthyl		5.2480	0.2735	0.59290	7098.77640	2.44579	1.91315	404.102	304.100
2p	8-Quinolyl		6.0809	0.1442	0.27442	4192.16360	1.97240	1.50397	372.917	363.920
	R <sup>c</sup>		-0.76	-0.75	-0.87	-0.77	-0.64	0.51	0.60	

\*\* = 2-(1-methyl-1H-imidazolyl).

<sup>a</sup> Mean values obtained from the PM3 single point conformations CSB set.<sup>b</sup> Mean values obtained from the STO-3G single point conformations CSC set.<sup>c</sup> R = correlation coefficient.

examples are included in Fig. 7, in which only the arylsulfonamide moiety is represented.

The data obtained show the LUMO 0 orbital located on the S and C atoms for all the analyzed compounds. These data, although they cannot be used as a discriminative value, suggest that the series **2** derivatives could undergo a nucleophilic interaction between a nucleophile agent and S, and it is expected that the bond cleavage will ultimately enable the release of **1a** proposed as the effective minimal fragment.

### 3. Conclusions

The data obtained in this study confirmed our initial hypothesis and allowed us to establish a preliminary correlation between the structure of the compounds, their conformational behavior, the proposed mechanism of action and the biological activity.

In fact, for active bis(phenyl) diselenide compounds in **1** series, such as **1a** and **1b**, the presence of the positive Se atoms in the central moiety of the molecular architecture, the geometric descriptor values adopted by the preferred conformations, and the location of the LUMO 0 over the central Se atoms, favor the idea that the preferred points for a nucleophilic attack might be the aforementioned atoms. This attack might result too in the cleavage of central Se<sub>1</sub>–Se<sub>2</sub> bond, and subsequently the possible release of the arylselenol, which can act in the redox system. The lower b.o. values calculated for the bond appear to support this proposal.

With respect to the bis(benzyl) diselenide derivatives, such as **1e** or **1o**, the location of the LUMO 0 orbital on the Se atoms suggests that these derivatives could also undergo the proposed nucleophilic attack, mediated by the residues present in the active site of the target enzymes; however, according to the bond order values obtained, the Se–Se bond cleavage is not expected for these compounds. The pattern of detected intramolecular hydrogen bonds and the H–arene and Se–heteroatom interactions for the preferred conformations suggest a larger exposure of the Se atoms in the most active compounds.

With respect to the sulfonamide derivatives belonging to the **2** series, they can be considered as molecular structures built on a common scaffold, bis(4-aminophenyl)diselenide, in which two aryl or heteroaryl fragments (monocyclic and bicyclic rings) are located on the scaffold nitrogen atoms. The aim of the designed structural variations was to evaluate the ability of these features to modulate the release of the compound **1a**, considered as the active moiety. In this way, the whole selenosulfonamide is considered as a pro-drug and the aromatic or heteroaromatic moieties as the release regulator elements.

With regard to the modulation of lipophilicity, achieved by the selected structural variations, a clear correlation between the solubility in water and the biological activity is detected.

Evaluation of the descriptors values that could be considered the most significant permits the proposal of a possible relationship among the polarizability, the molecular topology, shape and volume, and the biological activity that could be related with the accessibility of the cleavage points.

According to the proposed mechanism, a hydrolysis process can be mediated by the nucleophilic attack (a water molecule or another nucleophilic agent) on the sulfur atoms; the proposal appears to be supported by the larger positive atomic charges calculated for both atoms, and by the lower b.o. that is shown by S–N and S–C bonds in the sulfonamide moiety. In fact, it can be argued that when the nucleophilic attack on sulfur occurs, both S–N and S–C bonds are liable to break, with a possible preference for the latter bond. The preferred location of the LUMO 0 orbital over the target atoms also supports this approach.

The conformational behavior shown by these derivatives, preferably with a noteworthy pattern of intramolecular interactions, hydrogen bonds and H-arene, results in structural arrangements that facilitate the access of the nucleophilic agent, which causes the release of active moiety.

This last conclusion is supported by the interaction maps obtained and by the negative correlation detected among the biological activity and the topological descriptors that were calculated.

#### 4. Experimental

The calculations were performed on Dell Precision 380 workstations, provided with the Discovery Studio v2.5 suite, and on an SGI Virtu VS100 workstation, provided with Hyper-Chem v5 Pro, MOE2013.08, MOE2014 and MOPAC2009 software packages. Statistical calculations were performed using the statistical software UNStat, developed in the department of Biochemistry and Genetics of the Science School of the University of Navarra (<http://www.unav.edu/departamento/bioquimica-genetica/unstat-es>).

The reference compounds obtained from the Cambridge Structural Database, (CSD System version 5.35: search and information retrieval with ConQuest [76] version 1.16, structure visualization with Mercury [76] version 3.3), **DPHDE02** (selected as template for the M enantiomers) and **YUXPIR** (selected as template for the P enantiomers) were used as templates for building the initial models for the bisphenyldiselenide derivatives, whereas **HIRGIZ**, **YAWHEL**, **IXOYAW**, **DEMGIM**, and **KUZQUS** were selected as templates for the bisbenzyldiselenide derivatives.

The three-dimensional models of the studied compounds were constructed according to the initial configuration, in gas phase, using atoms from the corresponding module of the Discovery Studio v2.5 and using the implemented Dreiding force field. A preliminary optimization was carried out by applying the implemented Dreiding optimization engine with a root mean square gradient, rms, of 0.001 kcal/mol/Å<sup>2</sup> as completion criterion. Restraints and constraints were not applied.

The first minimized conformations obtained were considered as the starting conformations for the conformational analysis. The conformational search was carried out through a systematic search strategy with an rms gradient of 0.001 kcal/mol/Å<sup>2</sup>, an energy window of 5 kcal, and a maximum conformation number of 200. The resulting conformations (conformational set **CSA** for series 1 and **CSB** for series 2) were then optimized by applying the Dreiding minimize protocol implemented into the DS suite. Once the minimized conformations were obtained, we carried out a new selection choosing the lowest energy conformations included in an energy window of 5 kcal for each compound. The quantum analysis was carried out by applying the MOPAC2009 engine, using the PM3 semi-empirical approach, with a single point calculation carried out over the previously optimized Dreiding geometry, without further optimization.

The Interaction Potentials map that predicts the preferred location of O2H, NH, and O probes were calculated for the lowest

energy PM3 representative conformation (selected from the conformational ensemble 2b) by applying the calculation method implemented in the MOE2013.08 software suite. The contour map for O2H probe represents the interaction energy equal to -3.0 kcal/mol, whereas the NH and O maps represent the interaction energy equal to -2.5 kcal/mol.

With the conformations belonging to the **CSA** and **CSB** conformational sets, a small molecules database was constructed, using the MOE2014.09 software. The charge values were recalculated by the MOPAC engine implemented into the MOE2014, using the PM3 semi-empirical approach (single point). Next, the 2D and 3D descriptors selected from those available in the MOE2014 suite were calculated. The election of the descriptors is intended to cover a wide range of physical, topological and electrostatic properties. The script used for collecting and analyzing the data directly takes the values corresponding to the descriptors obtained, collected in the appropriate fields of the database; in this database, the 3D model for each conformation of each test compound is included in the model field. The remaining fields include all the descriptors. Data descriptors are directly exported to an Excel 2010 spreadsheet. For 2D MOE2014 descriptors, the data corresponding to a representative conformation of each of the compounds are taken. For conformation-dependent MOE2014 descriptors, the average values for each PM3 single point conformation is calculated (**CSA** and **CSB** sets).

The quantum PM3 descriptor parameters: atomic charges (Coulson type charges), HOMO and LUMO energies and the bond orders were calculated by applying the PM3 semi-empirical approach to the conformations included in the **CSA** and **CSB** sets. The data collected represent the average values for the conformations obtained. The polarizabilities were calculated with 0.0005 au force field strength. The locations of HOMO and LUMO orbitals were calculated on the representative lowest PM3 energy conformation.

For each compound of the **2** series, the five representative lowest PM3 energy conformations from each compound were selected (conformational set **CSC**) and a subsequent Ab initio analysis was carried out (STO-3G minimal basis set; RHF spin pairing and 0 total charge options, with a convergence limit of 1e-008 and 50 as the limit of number iteration). The mean polarizabilities were calculated with 0.0005 au force field strength.

A regression (*R*) analysis was carried out on the aforementioned descriptor set. The descriptors showing a value of *R* > 0.6 were selected. In order to reduce the dimensionality of the set of selected molecular descriptors; a Principal Components Analysis (PCA) was then applied, with a component limit equal to 3 and 80% of minimum variance.

#### Appendix A. Supplementary data

Supplementary data associated with this article can be found, in the online version, at <http://dx.doi.org/10.1016/j.jmgm.2015.06.002>

#### References

- [1] N.S. Akopyants, N. Kimblin, N. Secundino, R. Patrick, N. Peterson, P. Lawyer, D.E. Dobson, S.M. Beverley, D.L. Sacks, *Science* 324 (2009) 265–268, <http://dx.doi.org/10.1126/science.1169464>
- [2] U. Sharma, S. Singh, *J. Vector Borne Dis.* 45 (2008) 255–272.
- [3] Y.J.F. Garin, A. Sulahian, F. Pratlong, P. Menecur, J.P. Gangneux, E. Prina, J.P. Detet, F. Derouin, *Infect. Immun.* 69 (2001) 7365–7373.
- [4] J.H. Truppel, F. Otomura, U. Teodoro, R. Massafra, M.C.V. da Costa-Ribeiro, C.M. Catarino, L. Dalagranha, M.E.M.C. Ferreira, V. Thomaz-Soccol, *PLoS One* 9 (2014) e93731, <http://dx.doi.org/10.1371/journal.pone.0093731>
- [5] T.T. Guimarães, M.C.F.R. Pinto, J.S. Lanza, M.N. Melo, R.L. do Monte-Neto, I.M.M. de Melo, E.B.T. Diogo, V.F. Ferreira, C.A. Camara, W.O. Valenca, R.N. de

- Oliveira, F. Frézard, E.N. da Silva Jr, Eur. J. Med. Chem. 63 (2013) 523–530, <http://dx.doi.org/10.1016/j.ejmech.2013.02.038>
- [6] M.S. Klemper, T.R. Unnach, L.T. Hu, N. Engl. J. Med. 356 (2007) 2567–2569.
- [7] E. Mougnau, F. Bihl, N. Glaichenhaus, Immunol. Rev. 240 (2011) 286–296, <http://dx.doi.org/10.1111/j.1600-065X2010.00983.x>
- [8] F. Jeddi, C. Mary, K. Aoun, Z. Harrat, A. Bouratbine, F. Faraut, R. Benikhlef, C. Pomares, F. Pratlong, P. Marty, R. Piarroux, Antimicrob. Agents Chemother. 58 (2014) 4866–4874, <http://dx.doi.org/10.1128/AAC2521-13>
- [9] B. Rotureau, Med. Hypothe. 67 (2006) 1235–1241, <http://dx.doi.org/10.1016/j.mehy.2006.02.056>
- [10] P. Baiocco, G. Colotti, S. Franceschini, A. Ilari, J. Med. Chem. 52 (2009) 2603–2612, <http://dx.doi.org/10.1021/jm900185q>
- [11] K. Aït-Oudhia, E. Gazanion, B. Vergnes, B. Oury, D. Sereno, Parasitol. Res. 109 (2011) 1225–1232, <http://dx.doi.org/10.1007/s00436-011-2555-5>
- [12] T.P.C. Dorlo, M. Balasegaram, J.H. Beijnen, P.J. de Vries, J. Antimicrob. Chemother. 67 (2012) 2576–2597, <http://dx.doi.org/10.1093/jac/dks275>
- [13] F. Jeddi, R. Piarroux, C. Mary, J. Trop. Med. (2011) 695382, <http://dx.doi.org/10.1155/2011/695382>
- [14] D.C. Miguel, J.K. Yokoyama-Yasunaka, S.R. Uliana, PLoS Negl. Trop. Dis. 2 (2008) e249, <http://dx.doi.org/10.1371/journal.pntd.00000249>
- [15] T.S. Tiuman, A.O. Santos, T. Ueda-Nakamura, B.P. Filho, C.V. Nakamura, Int. J. Infect. Dis. 15 (2011) 525–532, <http://dx.doi.org/10.1016/j.ijid.2011.03.02>
- [16] R.L. Krauth-Siegel, O. Inhoff, Parasitol Res 90 (Suppl. 2) (2003) S77–S85.
- [17] B.C. Galarreta, R. Sifuentes, A.K. Carrillo, L. Sanchez, M.R.I. Amado, H. Maruenda, Bioorg. Med. Chem. 16 (2008) 6689–6695, <http://dx.doi.org/10.1016/j.bmc.2008.05.074>
- [18] M.C. Taylor, J.M. Kelly, C.J. Chapman, A.H. Fairlamb, M.A. Miles, Mol. Biochem. Parasitol. 64 (1994) 293–301.
- [19] S.F.P. Braga, E.V.P. Alves, R.S. Ferreira, J.R.B. Fradico, P.S. Lage, M.C. Duarte, T.G. Ribeiro, A.S. Polcarpo Jr, A.J. Romana, M.L. Tonini, M. Steindel, E.F. Coelho, R.B. de Oliveira, Eur. J. Med. Chem. 71 (2014) 282–289, <http://dx.doi.org/10.1016/j.ejmech.2013.11.011>
- [20] G.E. Linares, E.L. Ravaschino, J.B. Rodriguez, Curr. Med. Chem. 13 (2006) 335–360, <http://dx.doi.org/10.2174/092986706775476043>
- [21] Y. Zhang, C.S. Bond, S. Bailey, M.L. Cunningham, A.H. Fairlamb, W.N. Hunter, Protein Sci. 5 (1996) 52–61.
- [22] M. Deponte, Biochim. Biophys. Acta 1830 (2013) 3217–3266, <http://dx.doi.org/10.1016/j.bbagen.2012.09.018>
- [23] R.L. Krauth-Siegel, M.A. Comini, Biochim. Biophys. Acta 1780 (2008) 1236–1248, <http://dx.doi.org/10.1016/j.bbagen.2008.03.006>
- [24] C. Dumas, M. Ouellette, J. Tovar, M.L. Cunningham, A.H. Fairlamb, S. Tamar, M. Olivier, B. Papadopoulou, EMBO J. 16 (1997) 2590–2598, <http://dx.doi.org/10.1093/emboj/16.10.2590>
- [25] S. Krieger, W. Schwarz, M.R. Ariyanayagam, A.H. Fairlamb, R.L. Krauth-Siegel, C. Clayton, Mol. Microbiol. 35 (2000) 542–552, <http://dx.doi.org/10.1046/j.1365-2958.2000.01721.x>
- [26] R.L. Krauth-Siegel, S.K. Meiering, H. Schmidt, Biol. Chem. 384 (2003) 539–549, <http://dx.doi.org/10.1515/BC.2003.062>
- [27] G.A. Holloway, W.N. Charman, A.H. Fairlamb, R. Brun, M. Kaiser, E. Kostewicz, P.M. Novello, J.P. Paridot, J. Richardson, I.P. Street, K.G. Watson, J.B. Baell, Antimicrob. Agents Chemother. 53 (2009) 2824–2833, <http://dx.doi.org/10.1128/AAC1568-08>
- [28] R. Perez-Pineiro, A. Burgos, D.C. Jones, L.C. Andrew, H. Rodriguez, M. Suarez, A.H. Fairlamb, D.S. Wishart, J. Med. Chem. 52 (2009) 1670–1680, <http://dx.doi.org/10.1021/jm801306g>
- [29] K. Schwarz, C.M. Foltz, J. Am. Chem. Soc. 79 (1957) 3292–3293, <http://dx.doi.org/10.1021/ja01569a087>
- [30] J.T. Rotruck, A.L. Pope, H.A. Ganther, A.B. Swanson, D.G. Hafeman, W.G. Hoekstra, Science 179 (1973) 588–590, <http://dx.doi.org/10.1126/science.179.4073.588>
- [31] H. Tapiero, D.M. Townsend, K.D. Tew, Biomed. Pharmacother. 57 (2003) 134–144, [http://dx.doi.org/10.1016/S0753-3322\(03\)35-0](http://dx.doi.org/10.1016/S0753-3322(03)35-0)
- [32] H. Zeng, G.F. Combs Jr, J. Nutr. Biochem. 19 (2008) 1–7, <http://dx.doi.org/10.1016/j.jnutbio.2007.02.005>
- [33] N. Beheshti, S. Soflaei, M. Shakibaie, M.H. Yazdi, F. Ghaffarifar, A. Dalimi, A.R. Shahverdi, J. Trace Elem. Med. Biol. 27 (2013) 203–207, <http://dx.doi.org/10.1016/j.jtemb.2012.11.002>
- [34] M.A. Beck, O.A. Levander, J. Handy, J. Nutr. 133 (2003) 1463S–1467S.
- [35] H. Castro, F. Teixeira, S. Romao, M. Santos, T. Cruz, M. Flórido, R. Appelberg, P. Oliveira, F. Ferreira da Silva, A.M. Tomás, PLoS Pathog. 7 (2011) e1002325.
- [36] M.T.A. da Silva, I. Silva-Jardim, O.H. Thiemann, Curr. Med. Chem. 21 (2014) 1772–1780, <http://dx.doi.org/10.2174/0929867320666131119121108>
- [37] D. Moreno-Mateos, D. Plano, Y. Baquedano, A. Jiménez-Ruiz, J.A. Palop, C. Sanmartín, Parasitol. Res. 108 (2011) 233–239, <http://dx.doi.org/10.1007/s00436-010-2073-x>
- [38] D. Plano, Y. Baquedano, D. Moreno-Mateos, M. Font, A. Jiménez-Ruiz, J.A. Palop, C. Sanmartín, Eur. J. Med. Chem. 46 (2011) 3315–3323, <http://dx.doi.org/10.1016/j.ejmech.2011.04.054>
- [39] Y. Baquedano, E. Moreno, S. Espuelas, P. Nguewa, M. Font, K.J. Gutierrez, A. Jiménez-Ruiz, J.A. Palop, C. Sanmartín, Eur. J. Med. Chem. 74 (2014) 116–123, <http://dx.doi.org/10.1016/j.ejmech.2013.12.030>
- [40] H.M. Berman, J. Westbrook, Z. Feng, G. Gilliland, T.N. Bhat, H. Weissig, I.N. Shindyalov, P.E. Bourne, Nucl. Acids Res. 28 (2000) 235–242, <http://dx.doi.org/10.1093/nar/28.1.235>
- [41] S. Bailey, K. Smith, A.H. Fairlamb, W.N. Hunter, Eur. J. Biochem. 213 (1993) 67–75, <http://dx.doi.org/10.1111/j.1432-1033.1993.tb17734.x>
- [42] M. Goodarzi, E.F.F. da Cunha, M.P. Freitas, T.C. Ramalho, Eur. J. Med. Chem. 45 (2010) 4879–4889, <http://dx.doi.org/10.1016/j.ejmech.2010.07.060>
- [43] M.V. Papadopoulou, W.D. Bloomer, H.S. Rosenzweig, E. Chatelain, M. Kaiser, S.R. Wilkinson, C. McKenzie, J.-R. Isotet, J. Med. Chem. 55 (2012) 5554–5565, <http://dx.doi.org/10.1021/jm300508n>
- [44] C. Galiana-Rosello, P. Bilbao-Ramos, M.A. Dea-Ayuela, M. Roloín, C. Vega, F. Bolaíns-Fernández, E. García-España, J. Alfonso, C. Coronel, M.E. González-Rosende, J. Med. Chem. 56 (2013) 8984–8998, <http://dx.doi.org/10.1021/jm4006127>
- [45] P. Ruzza, A. Calderan, Pharmaceutics 5 (2013) 220–231, <http://dx.doi.org/10.3390/pharmaceutics5020220>
- [46] Accelrys Software Inc., Discovery Studio Modeling Environment Release 2.5. Accelrys Software Inc.: San Diego, USA, 2010.
- [47] Molecular Operating Environment (MOE), 2013.08 and 2014; Chemical Computing Group Inc., 1010 Sherbooke St. West, Suite #910, Montreal, QC, Canada, H3A 2R7, 2014.
- [48] HyperChem v5 Pro. Hypercube Inc. Gainesville, FL 32601 USA.
- [49] MOPAC MOPAC2009, Stewart, J.P. Stewart Computational Chemistry, Colorado Springs, CO, USA, <<http://OpenMOPAC.net>>, 2009.
- [50] F.H. Allen, Acta Cryst. B 8 (2002) 380–388, <http://dx.doi.org/10.1107/S0108768102003890>
- [51] A.L. Fuller, L.A.S. Scott-Hayward, Y. Li, M. Bühl, A.M.Z. Slawin, J.D. Woollins, J. Am. Chem. Soc. 132 (2010) 5799–5802, <http://dx.doi.org/10.1021/ja100247y>
- [52] F.H. Kruse, R.E. Marsh, J.D. McCullough, Acta Cryst. 10 (1957) 201, <http://dx.doi.org/10.1107/S0365110X5700064X>
- [53] G.D. Morris, F.W.B. Einstein, Acta Cryst. C42 (1986) 1433–1435, <http://dx.doi.org/10.1107/S0108270186092004>
- [54] G. Van Den Bossche, M.R. Spirlet, O. Dideberg, L. Dupont, Acta Cryst. C40 (1984) 1979–1980, <http://dx.doi.org/10.1107/S0108270184010301>
- [55] P.G. Jones, C. Kienitz, C. Thone, Z. Kristallogr. 209 (1994) 83, <http://dx.doi.org/10.1524/zkri.1994.209.1.83>
- [56] K. Helios, A. Pietraszko, W. Zierkiewicz, H. Wójcikowicz, D. Michalska, Polyhedron 30 (2011) 2466–2472, <http://dx.doi.org/10.1016/j.poly.2011.06.040>
- [57] K.P. Bhabak, G. Muges, Chem. Asian J. 4 (2009) 974–983, <http://dx.doi.org/10.1002/asia.200800483>
- [58] E.A. Meyers, R.A. Zingaro, N.L.M. Dereu, Z. Kristallogr. 210 (1995) 305, <http://dx.doi.org/10.1524/zkri.1995.210.4.305>
- [59] Y. Xu, Q.-C. Dong, H.-B. Tong, X.-H. Wei, Acta Cryst. (2007) E63:o4629, <http://dx.doi.org/10.1107/S1600536807055493>
- [60] M.-Y. Zhou, Y.-Q. Li, W.-J. Zheng, Acta Cryst. (2012) E68:o985, <http://dx.doi.org/10.1107/S1600536812007726>
- [61] H. Zhou, S.-Y. Ou, R.-A. Yan, J.-Z. Wu, Acta Cryst. (2011) E67:o19, <http://dx.doi.org/10.1107/S1600536811025736>
- [62] W.-J. Liu, M.-H. Wu, C.-Y. Bao, W.-D. Zou, X.-Y. Meng, Acta Cryst. (2006) E62:o3177–o3178, <http://dx.doi.org/10.1107/S1600536806024834>
- [63] G. Hua, A.L. Fuller, A.M.Z. Slawin, J.D. Woollins, Acta Cryst. (2010) E66:o2579, <http://dx.doi.org/10.1107/S1600536810036676>
- [64] S.L. Mayo, B.D. Olafson, W.A. Goddard, J. Phys. Chem. 94 (1990) 8897–8909.
- [65] J.J.P. Stewart, J. Comp. Chem. 12 (1991) 320–341, <http://dx.doi.org/10.1002/jcc.540120306>
- [66] I.V. Tetko, J. Gasteiger, R. Todeschini, A. Mauri, D. Livingstone, P. Ertl, V.A. Palyulin, E.V. Radchenko, N.S. Zefirov, A.S. Makarenko, V.Y. Tanchuk, V.V. Prokopenko, J. Comput. Aid. Mol. Des. 19 (2005) 453–463.
- [67] P.J. Goodford, J. Med. Chem. 28 (1985) 849–857, <http://dx.doi.org/10.1021/jm00145a002>
- [68] R.V. Hogg, E.A. Tanis, Probability and Statistical Inference, Prentice Hall, 2009.
- [69] CRC Handbook of Chemistry and Physics. CRC Press, (1994).
- [70] P. Labute, MOE LogP (Octanol/Water) Model unpublished. Source code in \$MOE/lib/svl/quasar.svl/q.logp.svl (1998).
- [71] L.H. Hall, L.B. Kier, Reviews of Computational Chemistry, Volume 2, In: B. Boyd, K. Lipkowitz (Eds.) (1991).
- [72] L.H. Hall, L.B. Kier, Eur. J. Med. Chem. – Chim. Therapeutica. 4 (1997) 307–312.
- [73] M. Petitjean, J. Chem. Inf. Comput. Sci. 32 (1992) 331–337, <http://dx.doi.org/10.1021/ci00008a012>
- [74] H. Wiener, J. Am. Chem. Soc. 69 (1947) 17–20, <http://dx.doi.org/10.1021/ja01193a005>
- [75] A.T. Balaban, Theor. Chim. Acta 53 (1979) 355–375.
- [76] I.J. Bruno, J.C. Cole, P.R. Edgington, M. Kessler, C.F. Macrae, P. McCabe, J. Pearson, R. Taylor, Acta Cryst. B 58 (2002) 389–397, <http://dx.doi.org/10.1107/S0108768102003324>.